Calcium-permeable AMPA receptors mediate timing-dependent LTP elicited by six coincident action potentials at Schaffer collateral-CA1 synapses

Running title: Modulation of threshold t-LTP

Efrain A. Cepeda-Prado[1], Babak Khodaie[1,3], Gloria D. Quiceno[1], Swantje Beythien[1], Volkmar Leßmann[1,2,3,Δ,*], Elke Edelmann[1,2,3*]

[1]Institut für Physiologie, Otto-von-Guericke-Universität, Medizinische Fakultät, Leipziger Str. 44, 39120 Magdeburg, Germany

[2]Center for Behavioral Brain Sciences, Magdeburg, Germany

[3]OVGU International ESF-funded Graduate School ABINEP, Magdeburg, Germany

* Shared senior authorship

[Δ] correspondence: lessmann@med.ovgu.de

Keywords:

spike timing-dependent plasticity, STDP, hippocampus, dopamine, calcium, BDNF, t-LTP

Abstract

Activity-dependent changes of synaptic transmission in neuronal circuits are thought to represent the cellular mechanism of memory formation in the brain. Experimentally, such changes can be elicited by repeated high-frequency synaptic stimulation inducing long-term potentiation (LTP), or by long-lasting low frequency stimulation, that induces long-term depression (LTD). In contrast, spike timing-dependent plasticity (STDP) can induce equally robust and long-lasting timing-dependent LTP (t-LTP) in response to low frequency repeats of coincident individual action potentials first in the presynaptic and then in the postsynaptic neuron. Conversely, this stimulation leads to t-LTD if the postsynaptic precedes the presynaptic action potential. Importantly, STDP is best suited to investigate synaptic plasticity mechanisms at the single cell level. Commonly, STDP paradigms relying on 25-100 repeats (comprising several minutes of synaptic stimulation) of coincident pre- and postsynaptic spike firing are used to elicit robust t-LTP or t-LTD. However, the minimum number of repeats required for successful STDP induction, which could account for single trial learning *in vivo* (comprising only a few seconds), is barely explored. Here, we examined low repeat STDP at Schaffer collateral-CA1 synapses by pairing one presynaptic action potential with either one postsynaptic action potential (1:1 t-LTP), or with a burst of 4 postsynaptic action potentials (1:4 t-LTP). Six repeats were sufficient to elicit 1:1 t-LTP while only three repeats were required for 1:4 t-LTP. Postsynaptic Ca^{2+} elevation for 1:1 t-LTP required Ca^{2+} influx via NMDARs and voltage gated calcium channels (VGCCs), but depended in case of 1:4 t-LTP on activation of metabotropic GluR and ryanodine receptor mediated Ca^{2+} release from internal stores. Surprisingly, both t-LTP variants were strictly dependent on a transient activation of postsynaptic Ca^{2+}-permeable AMPARs, although the locus of t-LTP expression was presynaptic for low repeat 1:1 t-LTP but depended on postsynaptic insertion of new GluA1 containing-AMPARs in case of low repeat 1:4 t-LTP. Both t-LTP forms were regulated differentially by dopamine receptor subtype 1 (D1R) and D2R activation, but occurred independent from BDNF/TrkB signaling. Our data suggest, that learning relevant long-lasting synaptic changes can be induced by only 3-6 repeats of mild STDP stimulation that can occur in < 10 s and could therefore underlie single trial learning *in vivo*.

54

55 Introduction

56

57 Long-term potentiation (LTP) and long-term depression (LTD) of synaptic transmission can be observed
58 in response to repetitive activation of synapses and are believed to represent cellular models of learning
59 and memory processes in the brain (see e.g., 1, 2, 3). While LTP leads to a stable enhancement of
60 synaptic transmission between connected neurons, LTD yields a long-lasting decrease in synaptic
61 responses. Depending on the time frame that is investigated, LTP as well as LTD can be divided into an
62 early phase lasting roughly 1h and a late phase that starts 2-3h after induction of the synaptic change.
63 While early LTP is mediated by posttranslational modifications, late LTP was found to depend on
64 synthesis of new proteins (4, but see 5). LTP was initially discovered using long-lasting high frequency
65 stimulation of glutamatergic synapses in the mammalian hippocampus (6), a brain region essential for
66 encoding episodic memory (7). While in these pioneering studies, LTP was recorded *in vivo* using
67 extracellular field potential recordings (6), LTP is also observed in acutely isolated brain slices *ex vivo*
68 and can be recorded in individual neurons using whole cell patch clamp recording techniques (reviewed
69 e.g. in 8, 9, 10). Notably, LTP studies at the single cell level are essential to understand the biochemical
70 and cellular mechanisms of LTP and LTD process.es of a specific neuronal connection with defined
71 postsynaptic target. To relate results from LTP measurements in acute slices *ex vivo* with learning
72 processes it is important to use LTP induction protocols that resemble synaptic activation patterns also
73 occurring during memory formation *in vivo* (compare 11), rather than paradigms involving tetanic
74 synaptic stimulation or long-lasting artificial depolarization of postsynaptic neurons.
75 In this respect, spike timing-dependent plasticity (STDP) seems to represent an especially relevant
76 protocol for induction of LTP (e.g., 12, 13-18). Here, bidirectional plasticity can be induced by repeated
77 coincident activation of pre- and postsynaptic neurons, with forward pairing (i.e. presynaptic spike
78 occurs several ms before the postsynaptic action potential; positive spike timing (+Δt)) yielding timing-
79 dependent (t-) LTP, while backward pairing (postsynaptic spike occurs before presynaptic activation; -
80 Δt) yields t-LTD. These protocols also fulfill the prerequisites for Hebbian synaptic plasticity (13) that are

81 widely accepted as fundamental requirements for synaptic strengthening. Compared to pairing
82 protocols that induce LTP by combining a presynaptic tetanus with a postsynaptic depolarization (e.g.,
83 19), STDP relies on a small number of pre- and postsynaptic action potentials that are repeated at low
84 frequency (< 5 Hz).
85 Like memory formation *in vivo*, t-LTP in acute *ex vivo* brain slices is strongly controlled by
86 neuromodulatory inputs (e.g., 20, 21-24, reviewed in 25). T-LTP was also reported to depend on brain-
87 derived neurotrophic factor signaling (e.g., 26, 27-30). Still, these mechanistic studies on t-LTP employed
88 STDP protocols depending typically on 25-100 repeats at ≤1 Hz that are unlikely to occur at synapses
89 during memory formation *in vivo*. Therefore, in the present study we started out to determine the
90 minimum number of repeats of coincident activation of pre- and postsynaptic neurons required for
91 successful t-LTP induction. To this aim, we used low repeat variants of our recently described canonical
92 (1:1 pairing: 22) and burst STDP protocols (1:4 pairing: 30). Although, STDP protocols involving low
93 repeat synaptic activation have been used previously to induce t-LTP (visual cortex: 31, cultured
94 hippocampal cells: 32, somatosensory cortex: 33, 34), the underlying cellular mechanisms for its
95 induction and expression remained elusive.
96 Our present study demonstrates, that Schaffer collateral (SC)- CA1 t-LTP can be induced robustly by only
97 six repeats of coincident pre- and postsynaptic spiking at 0.5 Hz. Moreover, our study reveals that,
98 depending on specific STDP paradigms (i.e. 1:1 vs. 1:4) the low repeat protocols recruit distinct sources
99 for postsynaptic Ca^{2+} elevation during induction of t-LTP, are mediated by distinct pre- and postsynaptic
100 expression mechanisms, and are differentially regulated by dopamine receptor signaling. Together
101 these data suggest that hippocampal SC-CA1 synapses can recruit multiple types of synaptic plasticity
102 in response to low repeat STDP protocols for processing of information and memory storage in the
103 hippocampus. Altogether, these distinct cellular STDP pathways might form the basis for the
104 pluripotency of hippocampal functions in learning and memory.
105
106 Results
107

108 Timing-dependent LTP at Schaffer collateral-CA1 synapses requires 3-6 spike pairings

109 Using whole cell patch clamp recordings, we investigated timing-dependent (t-)LTP at Schaffer collateral
110 (SC) -CA1 synapses in acute hippocampal slices obtained from juvenile (i.e. P28-35) male C57BL/6J mice.
111 T-LTP was induced by STDP protocols consisting of low repeat coincident pre- and postsynaptic action
112 potentials at low pairing frequencies (0.5 Hz).

113 SC-CA1 synapses were repeatedly activated by pairing of an excitatory postsynaptic potential (EPSP)
114 that was elicited by supra-threshold extracellular SC stimulation, with a single postsynaptically evoked
115 action potential (AP; 1EPSP/1AP or 1:1, Δt= 10 ms at 0.5 Hz; compare Fig. 1A). To determine the minimal
116 repeat number required for successful t-LTP induction with a prototypical STDP paradigm, neurons were
117 subjected to either 70, 50, 25, 12, 6, or 3 repeats of single spike pairings. Unexpectedly, we found that
118 just six spike pairings with 1:1 stimulation delivered at a frequency of 0.5 Hz were sufficient to induce
119 robust potentiation of EPSP slopes to 154.5% ± 8.2% at 30 min after induction. The t-LTP magnitude was
120 similar to the respective magnitude of t-LTP induced with either 25 or 70 repeats and significantly
121 different from negative controls (25 x: 145.4% ± 9.1% and 70 x: 166.9% ± 11.8; ANOVA $F_{(4,114)}$=4,8562
122 p=0.0012, posthoc Dunnet's Test: 70 x: p=0.0089; 25 x: p=0.0326, 6 x: p=0.0017, Fig 1A). Stimulation
123 protocols consisting of 6, 25 and 70 repeats produced slightly stronger effects than 12 or 50 x
124 stimulations (50 x: 137.5 ± 12.1% and 12 x: 146.1 ± 14.8%). However also t-LTP with 12 and 50 repeats
125 showed significant potentiation (50 x: 1-sample t-test $t_{(13)}$=3.092 p= 0.0086); 12 x: (1-sample t-test
126 $t_{(4)}$=3.350 p=0.0286). STDP experiments performed with 3 x 1:1 stimulation at 0.5 Hz, showed only a
127 very slight average increase of EPSP slopes to 104.6 ± 22.5% 30 min after induction that was highly
128 variable between cells. The average value was not significantly different from the respective EPSP slopes
129 observed after 40 min in control neurons that were not subjected to STDP stimulation (negative controls
130 (0:0): 105.0% ± 6.5%; Fig 1A). The time course of synaptic strength in an individual cell that was
131 potentiated with the low repeat 1:1 protocol is depicted at the right side in blue. These data indicate
132 that t-LTP can be induced at SC-CA1 synapses with low repeat t-LTP paradigms (i.e. 6 x 1:1), that might
133 more closely resemble the natural pattern of pre- and postsynaptic activity that can be observed during
134 memory formation in CA1 *in vivo* than any high frequency or high repeat LTP protocol.

Figure 1: Low repeat t-LTP at Schaffer collateral-CA1 synapses is dependent on stimulation pattern and on the repeat number. A) 1:1 t-LTP protocol consisting of the temporal coincident stimulation of an EPSP and one postsynaptic action potential (AP) with a time delay of +10 ms. Summary plot showing the average magnitude of t-LTP (EPSP slope normalized to baseline recording) in response to variable numbers of repeats of the 1:1 t-LTP protocol delivered at 0.5 Hz. Successful t-LTP could be induced with 6 (n= 56 / N= 44), 25 (n= 25 / N= 6) and 70 (n=10 / N=7) repeats of the 1:1 t-LTP protocol. Three repeats did not cause any changes in synaptic strength (n=7 / N=6), and showed similar normalized EPSP slopes as negative controls (0:0; n=23 / N=17). Right: original EPSPs and time course of 6 x 1:1 induced potentiation recorded in an individual representative cell example of a single STDP experiment performed for 6x 1:1 stimulation. **B)** 1:4 t-LTP protocol consisting of the temporal coincident stimulation of an EPSP and four postsynaptic action potentials (APs) with a time delay of +10 ms. Summary plot showing the average magnitude of t-LTP (EPSP slope normalized to baseline recording) in response to variable numbers of repeats of the 1:4 t-LTP protocol delivered at 0.5 Hz. Successful t-LTP could be induced with 3 (n=10 /N= 3), 6 (n=10 / N=6) and 35 (n=10 / N=8) repeats of the 1:4 t-LTP protocol. Two repeats did not cause changes in synaptic strength (n=10 /N =3) and showed similar normalized EPSP slopes as negative controls (0:0; n=8 / N=3). Right: original EPSPs and time course of 6 x 1:4 induced potentiation recorded in an individual representative cell. Averaged traces for EPSPs before and after LTP induction are shown as insets. * $p < 0.05$ ANOVA posthoc Dunnet's test. Data are shown as mean ± SEM.

Since it has been suggested, that successful induction of t-LTP at SC-CA1 synapses requires firing of multiple postsynaptic APs (35, 36), we incorporated a postsynaptic burst (4 APs delivered at 200 Hz) into the 6 x 1:1 protocol (Fig 1B). This protocol is referred to as 6 x 1EPSP/4AP (or 6 x 1:4, Fig 1B) paradigm and induced t-LTP at SC-CA1 synapses with the same efficiency as the 6 x 1:1 protocol (compare Fig 2C). As for the canonical protocol, we determined the threshold number of repeats also for the burst

161 protocol. As shown in Figure 1B, successful 1:4 t-LTP could be induced by only three repeats of our burst
162 protocol. Three, 6 and 35 repeats of 1:4 stimulation all yielded significant potentiation compared to the
163 negative control (0 x repeats; ANOVA $F_{(4,42)}$=9.3654 p<0.0001, posthoc Dunnett's Test: 3 x: p=0.0017; 6
164 x: p<0.0001; 35 x: 0.0415). The time course of change in synaptic strength of a typical cell obtained with
165 6 x 1:4 t-LTP stimulation is shown on the right. For further comparison and analysis of signaling and
166 expression mechanisms of t-LTP we focused in all subsequent experiments on the 6 repeat protocols
167 that induced with the same number of repeats successful t-LTP for both, the canonical and the burst
168 paradigm (indicated as 6 x 1:1 or 6 x 1:4).
169
170 Canonical and burst containing low-repeat STDP paradigms induce Hebbian t-LTP
171 When spike pairings were delivered with longer time delays between pre- and postsynaptic firing (Δt:
172 +20 ms) the magnitude of t-LTP declined (6 x 1:1: 132.1% ± 17.5% and 6 x 1:4: 118.3% ± 9.8). Stimulation
173 with short negative time delays (post-pre; Δt: -15 ms) did neither induce t-LTP nor significant t-LTD (6 x
174 1:1: 86.9% ± 9.6%; 6 x 1:4: 106.5 ± 10.5%; Fig 2A & B).
175
176 **Figure 2: Comparison of canonical and burst low repeat STDP paradigms.** STDP plots for 6 x 1:1 (**A**, blue)
177 and 6 x 1:4 (**B**, red) protocols. Changes in synaptic strength are shown for different intervals between
178 start of the EPSP and postsynaptic APs. Groups of cells at +10 ms interval (standard), with longer time
179 interval (+25 ms) or with negative spike pairings (-15 ms) are shown. Each open circle represents the
180 result for an individual CA1 neuron. Mean values are shown as closed circles. **C)** The time courses of t-
181 LTP expression do not differ between 6 x 1:1 (n= 56 / N= 44) and 6 x 1:4 (n= 34 / N= 27) paradigms, but
182 they were significantly different from negative controls (0:0; n= 23 / N= 17) and unpaired controls (6 x
183 0:4; n= 9 / N= 7). The average magnitude of t-LTP is shown in the bar graphs. **D)** Extended measurements
184 for 1 hour after t-LTP induction for both low repeat STDP protocols (6 x 1:1: n=6 / N=6, 6 x 1:4: n=9 /
185 N=8). Data are shown as mean ± SEM, bar scales are shown in the insets.
186

187 In general, the magnitude of t-LTP induced with the 6 x 1:4 stimulation (159.6% ± 8.0%) was comparable
188 to that observed for 6 x 1:1 stimulation (154.5% ± 8.2%; $p > 0.05$, compare Fig 2C). Eliciting only
189 postsynaptic bursts without pairing to presynaptic stimulation (6 x 0:4; 110.1 ± 11.9%) was not
190 significantly different from negative controls (0:0; 105.0% ± 6.5%, $p > 0.05$; Fig 2C). Importantly, these
191 results indicate that repeated postsynaptic burst firing alone does not induce any change in synaptic
192 strength. Prolonged patch clamp recordings carried out for 1 hour after pairing showed that both low
193 repeat STDP paradigms yielded at 60 min comparable t-LTP magnitudes as observed 30 min after
194 pairing. These data demonstrate that both low-repeat protocols enable longer lasting changes in
195 synaptic transmission without any decline in magnitude. Moreover, the overall time course of the
196 potentiation was indistinguishable for both types of low repeat t-LTP (Fig 2D). Together, these findings
197 indicate that the low repeat STDP paradigms identified in this study induce Hebbian plasticity selectively
198 at short positive spike timings with similar properties as has been described in earlier studies using high
199 repeat canonical and burst type STDP (e.g., 1, 30, 31).
200 In the next series of experiments, we determined the mechanisms of induction and expression as well
201 as the intracellular signaling cascades involved in modulation of both types of low repeat t-LTP.
202
203 Influence of single and multiple postsynaptic action potentials on t-LTP expression
204 To investigate whether the low repeat STDP paradigms introduced here, rely on pre- or postsynaptic
205 expression mechanisms of synaptic plasticity, we determined changes in the paired pulse ratio (PPR)
206 before and 30 min after t-LTP induction that was obtained when two successively evoked EPSPs were
207 elicited at 50 ms inter-stimulus interval (Fig. 3A). Commonly, a decrease in PPR after induction of LTP is
208 interpreted as an increase in transmitter release probability and would be expected in case of
209 presynaptically expressed synaptic plasticity. Interestingly, when t-LTP was induced with the 6 x 1:1
210 paradigm we found a significant increase rather than a decrease in PPR (paired Student's t-test, $t_{(28)}$
211 $=5.026$; $p<0.001$), whereas the PPR remained unchanged after inducing 6 x 1:4 t-LTP (paired Student's
212 t-test, $t_{(26)} = 1.066$; $p = 0.2960$; Fig 3A). This strong increase in PPR after induction of 6 x 1:1 t-LTP does
213 not directly hint at a presynaptic expression mechanism. However, it could be argued that the rise in

214 PPR under these conditions is due to an increase in the number of new effective release sites (i.e.
215 presynaptic unsilencing) with relatively low release probability. When determining PPR after induction
216 of t-LTP this would result in a small EPSP in response to the first pulse that becomes much larger in
217 response to the second PPR stimulus (see 37, 38). Accordingly, the data shown in Figure 3A might still
218 be consistent with presynaptic expression of 6 x 1:1 t-LTP. In contrast, the PPR analysis clearly speaks
219 against any presynaptic contribution in the expression of 6 x 1:4 t-LTP. Interestingly, the initial PPR
220 before inducing t-LTP was not significantly different between the tested groups (negative control (0:0):
221 1.77 ± 0.09; 6 x 1:1: 1.78 ± 0.08; 6 x 1:4: 1.74 ± 0.06; Kruskal-Wallis test, $H_{(2)} = 0.059$; $p = 0.9710$),
222 indicating that the initial release probability was similar and a stable basal parameter in our slices.
223
224 **Figure 3: Different loci of expression for t-LTP induced by the low repeat 1:1 and 1:4 paradigms.** A)
225 Paired pulse ratio (PPR) calculated before (pre-cond.) and after (post-cond.) t-LTP induction, or at the
226 beginning and the end of measurements in negative controls (0:0: n=18/N= 16; 6 x 1:1: n=29/N= 24; 6
227 x 1:4: n=31/N=23 animals). B) Right: original traces of AMPAR mediated currents recorded in voltage
228 clamp at -70 mV holding potential (Vm) and NMDAR (gray) mediated currents at -20 mV holding
229 potential. Left: ratio of AMPA/NMDA receptor mediated currents (AMPAR: peak current at -70 mV;
230 NMDAR: current amplitude 50 ms after start of EPSC, recorded at -20 mV) for negative controls (0:0;
231 n=12 / N= 9) and after induction of t-LTP with both low repeat paradigms (6 x 1:1: n= 12 / N=11; 6 x 1:4:
232 n= 7 / N= 5). C) Intracellular application of Pep1-TGL (inhibiting membrane insertion of GluA containing
233 AMPARs) blocks 6 x 1:4 t-LTP, whereas 6 x 1:1 t-LTP remains intact (6 x 1:1: ACSF; n= 12 / N= 10, Pep1-
234 TGL n= 9 / N= 7 and 6 x 1:4: ACSF n= 11 / N= 11, Pep-TGL n= 9 / N= 7). Data are shown as mean ± SEM.
235 Scale bars are shown in the figures.
236
237 To further address the locus of expression of 6 x 1:1 and 6 x 1:4 t-LTP, we analyzed the changes in
238 AMPA/NMDA receptor (R) mediated current ratios 30 min after inducing t-LTP. This analysis revealed a
239 strong and statistically significant increase in AMPAR vs. NMDAR-mediated excitatory postsynaptic
240 currents (EPSCs) following the induction of 6 x 1:4 t-LTP but not when inducing 6 x 1:1 t-LTP, or in non-

241 STDP stimulated control cells (ANOVA $F_{(2, 34)} = 7.979$; $p = 0.0014$, Fig 3B). Since an increase in
242 AMPAR/NMDAR mediated currents after inducing LTP is commonly explained by the insertion of new
243 GluA1 containing AMPARs into the postsynaptic spine (30, 39-41) these data strongly suggest a
244 postsynaptic mechanism of expression selectively for the 6 x 1:4 t-LTP.
245 As the next step, we asked whether this postsynaptic mechanism is driven specifically by incorporation
246 of GluA1 containing AMPARs. To investigate whether 6 x 1:4 stimulation leads to the insertion of GluA1
247 containing AMPARs, we loaded the postsynaptic cells with Pep1-TGL via the patch pipette solution and
248 induced t-LTP with both 6 repeat t-LTP paradigms (compare 30). Pep1-TGL contains the last three amino
249 acids of the C-terminus of the GluA1 subunit, which are required for its insertion into the plasma
250 membrane (42, 43). The postsynaptic application of Pep1-TGL resulted in a complete block of 6 x 1:4 t-
251 LTP (Mann-Whitney U test, $U = 14.0$; $p = 0.007$). In contrast, t-LTP induced with the 6 x 1:1 protocol
252 remained intact under the same recording conditions (Mann-Whitney U test, $U = 36.0$; $p = 0.201$, Fig
253 3C). Together with the PPR analysis and the AMPA/NMDAR ratios, these data suggest a prevailing
254 presynaptic locus of expression for the 6 x 1:1 t-LTP, and a dominant postsynaptic locus of expression
255 for the 6 x 1:4 stimulation induced synaptic plasticity. These findings are consistent with our previous
256 results obtained with high repeat t-LTP protocols (30). The data suggest that the number of postsynaptic
257 spikes fired during induction of low repeat t-LTP decides whether associative Hebbian synaptic plasticity
258 is expressed by pre- or by postsynaptic mechanisms, whereas the locus of t-LTP expression does not
259 seem to depend on the number of repeats of a specific t-LTP paradigm.
260

261 **Distinct calcium sources are recruited for induction of low repeat STDP paradigms**

262 There is a general consensus that induction of long-lasting changes in synaptic strength at SC-CA1
263 synapses requires a postsynaptic rise in intracellular calcium concentration ($[Ca^{2+}]_i$) via NMDA receptors
264 (NMDARs, 44). Likewise, also intracellular Ca^{2+} elevation resulting from synchronous activation of
265 NMDARs, voltage-gated Ca^{2+} channels (VGCC), and release of Ca^{2+} from internal stores, together with
266 activation of metabotropic glutamate receptors (mGluRs) might be responsible for postsynaptic STDP
267 induction (45). Accordingly, we investigated the sources for the intracellular Ca^{2+} elevation triggering

268 the 6 x 1:1 and 1:4 t-LTP. Interestingly, the 6 x 1:1 t-LTP was significantly impaired when it was executed
269 either in the presence of the specific NMDAR antagonist APV (50 µM; unpaired Student's t-test, $t_{(26)}$ =
270 2.348; p = 0.0268 ; Fig 4A), or in the presence of the L-type VGCC blocker Nifedipine (25 µM; unpaired
271 Student's t-test, $t_{(14)}$ = 4.25; p = 0.0008; Fig 4C). In contrast, neither APV (50 µM, unpaired Student's t-
272 test, $t_{(22)}$ = 1.016; p = 0.3207; Fig 4B) nor Nifedipine (25 µM, Mann-Whitney U test, U = 20.0; p =0.6620,
273 Fig 4D) inhibited t-LTP induced with the 6 x 1:4 protocol. These data indicate that postsynaptic Ca^{2+} influx
274 via NMDAR and VGCC is required for 6 x 1:1 but not for 6 x 1:4 t-LTP induction.
275
276 **Figure 4: Contribution of NMDA receptors and VGCCs to the induction of 6 x 1:1 and 6 x 1:4 t-LTP.** Effects
277 of bath applied NMDAR antagonist APV (50 µM) and L-type voltage-gated calcium channel (VGCC)
278 inhibitor Nifedipine (25 µM) on low repeat t-LTP. Inhibition of either NMDAR or VGCC activation
279 completely blocked 6 x 1:1 t-LTP (**A)** 6 x 1:1: ACSF n=14 / N=8, APV n= 13 / N= 12 and **C)** DMSO control
280 n= 8 / N=7, Nifedipine n=8 / N=7), whereas 6 x 1:4 t-LTP remained unaffected (**B)** 6 x 1:4: ACSF n=10 /
281 N=6, APV n=14 / N=9; **D)** DMSO n=8 / N=4, Nifedipine n=6 / N=4). Average time course of potentiation
282 and mean (± SEM) magnitude of t-LTP are shown for the respective experiments.
283
284 To verify a role of postsynaptic Ca^{2+} signaling in the induction of 6 x 1:4 t-LTP, we loaded postsynaptic
285 neurons with 10 mM of the Ca^{2+} chelator BAPTA via the patch pipette solution (Fig 5A). After obtaining
286 the whole cell configuration, the BAPTA containing internal solution was allowed to equilibrate for 30
287 min before t-LTP induction. As shown in figure 5A, buffering of intracellular Ca^{2+} signals in this way
288 resulted in a complete impairment of 6 x 1:4 t-LTP (Mann-Whitney U test, U = 3.0; p =0.0303), indicating
289 that a rise in postsynaptic $[Ca^{2+}]_i$ is indeed required also for the induction of 6 x 1:4 t-LTP.
290
291 **Figure 5: Contribution of group I mGluR and ryanodine receptor-dependent calcium release from**
292 **internal stores to 6 x 1:4 t-LTP**. **A)** Inclusion of 10 mM BAPTA in the intracellular solution prevented t-
293 LTP induced by 6 x 1:4 stimulation (Control: n=5 / N=5, $BAPTA_i$: n=6 / N=4), indicating the necessity of
294 postsynaptic calcium elevation to induce t-LTP. **B)** T-LTP induced with the 6 x 1:4 protocol was neither

295 affected by bath application of the mGluR1 antagonist YM-298198 (1 µM; ACSF: n=7 / N=5, YM-298198:
296 n=6 / N=3), nor by the mGluR5 antagonist MPEP (10 µM, n=6 / N=4). **C)** However, co-application of both
297 antagonists (YM-298198 and MPEP; ACSF n=12 / N=8, YM-MPEP n=12 / N=5) significantly reduced
298 synaptic potentiation. **D)** Wash in of 100 µM ryanodine into the postsynaptic neuron via the patch
299 pipette inhibited t-LTP induced by 6 x 1:4 stimulation (DMSO n= 9 / N= 4; Ryanodine n= 14 / N= 5).
300 Average time course of potentiation and mean (± SEM) magnitude of t-LTP are shown for the respective
301 experiments.
302
303 Since induction of t-LTP involves repeated glutamate release that should contribute to the induction
304 process, we next tested the involvement of metabotropic glutamate receptors (mGluRs) in 6 x 1:4 t-LTP.
305 In the hippocampal CA1 region $mGluR_1$ and $mGluR_5$ are widely expressed and have been reported to
306 facilitate Ca^{2+} release from internal calcium sources during LTP (e.g., 5, 46, 47). Nevertheless, blocking
307 mGluR activation by bath application of antagonists of either $mGluR_1$ (YM198298, 10 µM) or $mGluR_5$
308 (MPEP, 10 µM) alone, did not affect the magnitude of 6 x 1:4 t-LTP compared to ACSF controls (Kruskal-
309 Wallis test, $H_{(2)} = 0.2774$; $p = 0.8705$; Fig 5B). However, coapplication of the $mGluR_1$ and $mGluR_5$
310 antagonists significantly impaired the 6 x 1:4 t-LTP (unpaired Student's t-test, $t_{(22)} = 2.248$; $p = 0.0093$;
311 Fig 5C), indicating that the activation of one of these receptors alone (either $mGluR_1$ or $mGluR_5$) is
312 sufficient and required to support 6 x 1:4 t-LTP.
313 To test for involvement of internal Ca^{2+} stores in the low repeat burst protocol, we applied 100 µM
314 ryanodine (a concentration known to irreversibly inhibit RyR; 48) via the patch pipette into the recorded
315 postsynaptic neurons. As expected in case of RyR involvement, 6 x 1:4 t-LTP induction was completely
316 inhibited under these conditions (Mann-Whitney U test, U= 5.5; p = 0.0003; Fig 5D). These data indicate
317 that Ca^{2+} release from the ER is a critical component of 6 x 1:4 t-LTP. Thus, the postsynaptic Ca^{2+}
318 elevation required for induction of 6 x 1:4 t-LTP seems to involve $mGluR_1$ or $mGluR_5$ mediated release
319 of Ca^{2+} from the ER via IP3 receptors and subsequent Ca^{2+} induced Ca^{2+} release via RyRs.
320

321 **Distinct dopaminergic modulation of different low repeat t-LTP protocols at Schaffer collateral-CA1**
322 **synapses**

323 Dopamine (DA) serves as an important neuromodulator in learning and memory formation, as well in
324 synaptic plasticity mechanisms underlying both phenomena. DA receptors in the brain are classified into
325 two main families: D1-like receptors that include D1 and D5, and D2-like receptors that include D2, D3
326 and D4 (49). It has been shown that activation of D1/D5 receptors has a particularly strong influence on
327 synaptic efficacy (e.g., 50, 51), and that treatment of cultured hippocampal neurons with exogenous DA
328 (20 µM) reduces the induction threshold for t-LTP from 60 to 10 spike pairings (32). To examine whether
329 in our case, endogenous DA signaling is an essential component of synaptic mechanisms triggering low
330 repeat t-LTP, we investigated the effect of specific bath applied antagonists for D1-like and D2-like DA
331 receptors (D1: SCH23390 (SCH), 10 µM; D2: Sulpiride (Sulp), 10 µM). We found that t-LTP induced with
332 6 x 1:1 stimulation was blocked completely when SCH23390 and Sulpiride were coapplied (Kruskal-
333 Wallis test, $H_{(3)} = 14.28$; $p = 0.003$), whereas application of either the D1-like or the D2-like receptor
334 antagonist alone did not significantly reduce the magnitude of the 6 x 1:1 t-LTP (Fig 6A). In contrast, the
335 6 x 1:4 t-LTP was dependent exclusively on D2-like receptor signaling, as was evident from complete
336 inhibition of this burst t-LTP in the presence of Sulpiride (significantly different from ACSF controls;
337 Kruskal-Wallis test $H_{(3)} = 12.65$; $p = 0.005$, Fig 6B), whereas SCH23390 was without effect.

338

339 **Figure 6: Differential modulation of canonical and burst low repeat t-LTP by dopaminergic signaling. A)**
340 Dependence of 6 x 1:1 t-LTP on D1 and D2 receptor signaling. Neither bath application of SCH23390
341 (SCH, D1-like antagonist; 10 µM) nor bath application of Sulpiride (Sulp, D2-like antagonist; 10 µM) alone
342 impaired t-LTP (ACSF: n=12 / N=9; SCH23390 n=9 / N=6; Sulpiride n=10 / N=8). However, co-application
343 of both antagonists significantly reduced t-LTP (SCH + Sulp n=9 / N=4). **B)** T-LTP induced with the 6 x 1:4
344 protocol was impaired in the presence of Sulpiride, but not further reduced by co-application with
345 SCH23390. Accordingly, application of SCH23390 alone did not affect 6 x 1:4 t-LTP (ACSF: n=9 / N=6;
346 SCH23390 n=10 / N=5; Sulpiride n=11 / N=8; SCH + Sulp n=7 / N=4). **C)** T-LTP induced with the high
347 repeat (70 x) 1:1 protocol was inhibited in the presence of the D1 receptor antagonist SCH23390 (10

348 µM) in mouse slices (ACSF n=10 / N=8; SCH23390 n=14 / N=5) to a similar extent as observed previously
349 in rat hippocampal slices (Edelmann and Lessmann, 2011). Average time course of potentiation and
350 mean (± SEM) magnitude of t-LTP are shown for the respective experiments.
351
352 Together, these data indicate that 6 x 1:1 t-LTP depends on D1/D2 receptor co-signaling whereas 6 x
353 1:4 t-LTP is only dependent on D2 receptors, highlighting an important role of D2 receptors in both types
354 of t-LTP. This is at variance with the fact that most previous studies investigating DA-dependent LTP at
355 SC-CA1 synapses reported an eminent role of D1-like receptors (e.g., 51, 52). A similar role for D1
356 receptor signaling was also described for for high repeat (70 x) canonical t-LTP in rat hippocampal slices
357 (22, 23). To clarify whether repeat number or species matter for the contribution of D1 and D2 receptors
358 in t-LTP, we re-examined DA dependence of high repeat 70 x 1:1 t-LTP in mouse hippocampal slices. We
359 found that also in mouse slices 70 x 1:1 t-LTP was fully blocked by bath application of the D1 antagonist
360 SCH23390 (unpaired Student's t-test, $t_{(22)} = 3.028$; $p = 0.0062$; Fig 6C). These data reveal that high repeat
361 number induced t-LTP is regulated by D1 signaling whereas D2 signaling is selectively involved in low
362 repeat t-LTP. Further, the extent of D2 receptor involvement in low repeat t-LTP is regulated by the
363 postsynaptic spike pattern used for t-LTP induction.
364
365 The role of BDNF/TrkB signaling in low repeat t-LTP induced by canonical or burst protocols
366 We recently showed for SC-CA1 synapses that brain-derived neurotrophic factor (BDNF) induced
367 tropomyosin related kinase B (TrkB) signaling mediates t-LTP elicited by a 1:4 t-LTP paradigm with 25
368 repeats at 0.5 Hz. This t-LTP is driven by an autocrine postsynaptic BDNF/TrkB mechanism that relies on
369 postsynaptic insertion of new AMPA receptors (30). To investigate the role of BDNF/TrkB signaling in
370 synaptic plasticity processes induced with low repeat t-LTP protocols, we first tested whether bath
371 application of the non-selective tyrosine kinase inhibitor K252a has an effect on low repeat t-LTP. In the
372 presence of 200 nM K252a, a concentration that is commonly used to block Trk receptor signaling, 6 x
373 1:1 t-LTP was inhibited (Mann-Whitney U test, $U = 37.0$; $p = 0.0306$), whereas K252a had no effect on 6
374 x 1:4 t-LTP (Mann-Whitney U test, $U = 19.0$; $p = 0.9433$; Fig 7A). To address whether release of

375 endogenous BDNF might be involved in low repeat t-LTP, we next tested our low repeat t-LTP protocols
376 in slices obtained from heterozygous BDNF knockout ($BDNF^{+/-}$) mice which express ~50% of BDNF
377 protein levels compared to WT littermates (e.g., 53, 54; Fig7B). Our results show that both types of low
378 repeat t-LTP remained functional in response to this chronic depletion of BDNF (6 x 1:1 t-LTP: Mann-
379 Whitney U test, U = 25.0; p = 0.7789; and 6 x 1:4 t-LTP: Mann-Whitney U test, U = 14.0; p = 0.5887, Fig
380 7B). Finally, to examine whether acute inhibition of BDNF/TrkB signaling affects low repeat t-LTP, we
381 asked whether scavenging of BDNF by bath applied TrkB receptor bodies (human TrkB-Fc chimera, TrkB-
382 Fc) impairs canonical or burst low repeat t-LTP (Fig 7C). However scavenging of BDNF had no effect on
383 the magnitude of t-LTP induced by either of the two protocols (6 x 1:1 t-LTP: Mann-Whitney U test, U =
384 13.0; p = 0.0939 and 6 x 1:4 t-LTP: Mann-Whitney U test, U = 22.0; p = 0.8048, Fig 7C).
385
386 **Figure 7: BDNF induced TrkB receptor signaling is not required for t-LTP elicited by low repeat t-LTP**
387 **protocols. A)** The 6 x 1:1 t-LTP was inhibited by bath application of the tyrosine kinase inhibitor K252a
388 (200 nM; left), while t-LTP induced with the 6 x 1:4 paradigm (right) remained unaffected (6 x 1:1: DMSO
389 n=14 / N=10, K252a n=10 / N=7; 6 x 1:4: DMSO n=5 / N=4, K252a n=9 / N=6). **B)** Low repeat t-LTP was
390 not different for 6 x 1:1 (left) and 6 x 1:4 (right) stimulation in heterozygous BDNF knockout animals ($^{+/-}$)
391 compared to wild type litter mates (6 x 1:1: +/+ n 7 / N=6, +/- n=8 / N=7; 6 x 1:4: +/+ n=6 / N=5, +/- n=6
392 / N=5). **C)** Bath application of the BDNF scavenger TrkB-Fc (100 ng/ml; 3h preincubation) did not affect
393 t-LTP in response to the two low repeat protocols (left: 6 x 1:1: ACSF n=7 / N=5, TrkB-Fc n=6 / N=6; right:
394 6 x 1:4: ACSF n=7 / N=5, TrkB-Fc n= 7 / N= 6). Average time course of potentiation and mean (± SEM)
395 magnitude of t-LTP are shown for the respective experiments.
396
397 Together these data suggest that 6 x 1:4 t-LTP is independent from BDNF induced TrkB signaling, and
398 that the 6 x 1:1 t-LTP might involve TrkB receptor signaling, but is clearly not dependent on
399 endogenously released BDNF. In conjunction with our previous observation that 25 x 1:4 t-LTP is
400 dependent on release of endogenous BDNF (compare 30) the present data suggest that a higher
401 number (>6) of postsynaptic bursts in the t-LTP protocol is required to activate BDNF secretion. It could

402 be argued, that inhibition of 6 x 1:1 t-LTP in the presence of K252a results from a block of TrkB receptor
403 transactivation, which is stimulated by zinc influx through NMDA receptors (compare 55, but see 56,
404 57). However, when Zn^{2+} influx was blocked in the presence of the bath applied zinc chelator TPEN (10
405 µM), the 6 x 1:1 t-LTP was still functional (6 x 1:1: DMSO: 173.7 ± 24.8; TPEN: 208.7 ± 35.6; Mann-
406 Whitney U test, U = 22.0; p =0.5358).
407 Overall these experiments show that BDNF induced TrkB receptor signaling is not involved in either of
408 the two low repeat t-LTP protocols in investigated here.
409
410 The role of GluA2-lacking, calcium-permeable AMPA receptors in low repeat t-LTP
411 Recently, the transient incorporation of GluA2-lacking, Ca^{2+} permeable (cp-) AMPARs after LTP induction
412 has been proposed as an important process to increase postsynaptic Ca^{2+} for LTP expression (58-60,
413 reviewed in 61). To examine whether these receptors are involved in low repeat t-LTP, we incubated
414 our recorded hippocampal slices with the selective cp-AMPAR inhibitor NASPM (100 µM). Interestingly,
415 6 x 1:1 t-LTP and 6 x 1:4 t-LTP were both completely blocked in the presence of NASPM (6 x 1:1: unpaired
416 Student's t-test, $t_{(12)} = 3.257$; p= 0.0069; 6 x 1:4: unpaired Student's t-test, $t_{(11)} = 3.330$; p= 0.0067, Fig
417 8A & B). Surprisingly, these results indicate that the influx of Ca^{2+} via GluA2-lacking, cp-AMPARs is
418 mandatory to elicit low-repeat t-LTP induction.
419
420 **Figure 8: Ca^{2+} influx via GluA2-lacking calcium-permeable AMPARs is required for low-repeat t-LTP**
421 **induction.** Bath application of a selective inhibitor of Ca^{2+} permeable AMPARs (100 µM NASPM) blocks
422 6 x 1:1 t-LTP (**A)** as well as 6 x 1:4 t-LTP (**B**; 6 x 1:1: ACSF n=7 / N=4, NASPM n=7 / N=3; 6 x 1:4: ACSF n=
423 6 / N=4, NASPM n=7 / N=3). Average time course of potentiation and mean (± SEM) magnitude of t-LTP
424 are shown for the respective experiments. **C)** Successful induction of 6 x 1:1 t-LTP and subsequent 6 x
425 1:4 t-LTP in the same cells (n=6 / N=3). Note the absence of any signs of occlusion between t-LTP induced
426 by the two low repeat protocols.
427

428 In light of the many differences in the induction, expression mechanisms, and dopaminergic modulation
429 of the canonical 6 x 1:1 t-LTP and the 6 x 1:4 burst t-LTP we asked whether both types of t-LTP can be
430 elicited completely independent from one another or if they occlude each other. To this aim, we first
431 induced 6 x 1:1 t-LTP followed in the same cells by a subsequently induced 6 x 1:4 t-LTP. As shown in
432 figure 8C, both types of t-LTP could be activated independently without any signs of occlusion. Given
433 the strong differences in the induction processes and the presynaptic expression of 6 x 1:1 vs.
434 postsynaptic expression of 6 x 1:4 t-LTP, this absence of occlusion was an expected finding. However,
435 this result corroborates the independence of the two different types of low repeat t-LTP investigated
436 here.
437
438 The scheme presented in figure 9 summarizes our findings for the presynaptically expressed 6 x 1:1 t-
439 LTP and the postsynaptically expressed 6 x 1:4 t-LTP and suggest the putative roles of mGluRs, cp-
440 AMPARs, dopamine signaling, and internal Ca^{2+} stores in low repeat t-LTP. However, since the
441 distribution of dopaminergic fibers and the pre- and/or postsynaptic dopamine receptor localization in
442 the CA1 region and is not yet clear (compare 25), further experiments are clearly required to improve
443 the mechanistic understanding of this aspect of low repeat t-LTP. None withstanding, both low repeat
444 t-LTP forms are already by now clearly distinguishable. Their different features of induction and
445 expression mechanisms and the distinct signaling cascades they employ likely form the basis for the
446 versatile computing capacity of individual neurons.
447
448 **Figure 9: Suggested cellular signaling mechanisms involved in low repeat t-LTP at Schaffer collateral-CA1**
449 **synapses.** Summary of induction, signaling, and expression mechanisms involved in low repeat canonical
450 (i.e. 6 x 1:1 t-LTP) and burst (i.e. 6 x 1:4) t-LTP protocols in CA1 pyramidal neurons. **A)** Synaptic
451 mechanisms involved in the presynaptically expressed 6 x 1:1 t-LTP. T-LTP induction depends on
452 postsynaptic NMDAR and L-type VGCC mediated Ca^{2+} influx (1.). Insertion of cp-AMPARs into the
453 postsynaptic membrane might be regulated by D1/D2 signaling (2.) and could account for the combined
454 D1/D2 receptor dependence of 6 x 1:1 t-LTP. Ongoing low frequency test stimulation after induction of

455 t-LTP leads to sustained Ca^{2+} elevations through postsynaptic cp-AMPARs (3.). The resulting prolonged
456 postsynaptic Ca^{2+} elevation leads via a yet unidentified retrograde messenger to increased presynaptic
457 efficacy (4.). An additional presynaptic contribution of D1/D2 signaling to enhanced presynaptic
458 glutamatergic function is possible. **B)** The postsynaptically expressed 6 x 1:4 t-LTP does neither require
459 postsynaptic NMDAR nor L-type VGCC activation for induction. It rather depends on calcium release
460 from postsynaptic internal stores mediated by $mGluR_{1,5}$-dependent activation of IP3 receptors in the ER
461 (1.). This initial postsynaptic Ca^{2+} rise is amplified by Ca^{2+} dependent Ca^{2+} release via Ryanodine
462 receptors (RyRs; 2.). Moreover, the 6 x 1:4 t-LTP depends (like 6 x 1:1 t-LTP) on the activation of cp-
463 AMPARs. Intact D2 receptor signaling is mandatory to observe 6 x 1:4 t-LTP and might be involved in
464 recruiting cp-AMPARs to the postsynaptic membrane (3.) for sustained Ca^{2+} influx during ongoing low
465 frequency synaptic stimulation after t-LTP induction (4.). The resulting prolonged postsynaptic Ca^{2+}
466 elevation initiated by mGluRs, RyRs, and cp-AMPARs leads to postsynaptic expression of 6 x 1:4 t-LTP by
467 insertion of new GluA1 and GluA2-containing AMPARs into the postsynaptic membrane (5.)
468
469
470

471 Discussion

472 Our study shows that t-LTP at hippocampal SC-CA1 synapses requires only six repeats of coincident
473 presynaptic stimulation paired with either 1 or 4 postsynaptic spikes at low frequency (0.5 Hz). For the
474 1:4 burst protocol, even just three repeats are sufficient to elicit t-LTP. The 6 x 1:1 t-LTP could be induced
475 by Ca^{2+} influx via postsynaptic NMDARs and VGCCs, occurred independent of BDNF release, and
476 required combined D1/D2 receptor signaling. In contrast, the 6 x 1:4 t-LTP was induced by postsynaptic
477 Ca^{2+} release from internal stores mediated via mGluRs and ryanodine receptors, occurred independent
478 from BDNF/TrkB signaling, and was completely inhibited in the presence of D2 receptor antagonists.
479 Both, low repeat canonical and burst t-LTP, strongly depended on activation of GluA2-lacking cp-
480 AMPARs. These data suggest that low repeat STDP paradigms with potentially high physiological
481 relevance can induce equally robust t-LTP as observed for high repeat t-LTP in the hippocampus.
482 However, the pharmacological profile of low repeat t-LTP induction and expression revealed
483 astonishingly subtle differences between both induction protocols.

484

485 Dependence of t-LTP on repeat number and frequency of the STDP stimulation

486 Both 6 x t-LTP protocols used in our study yielded robust t-LTP with similar time courses as described
487 previously for standard STDP paradigms that used either higher number of pairings or higher pairing
488 frequency (compare e.g., 20, 30, 45, 62, 63-65). To date, only few studies focused on STDP protocols
489 with low numbers of repeats for t-LTP induction (discussed in 17, 31, 32, 34). Since only such low repeat
490 t-LTP protocols can be completed within a few seconds, these protocols are likely to represent a very
491 physiological model for synaptic plasticity events triggering learning and memory processes that can
492 also occur on a timescale of seconds. Thus, investigating the underlying signaling mechanisms appears
493 to be relevant for learning induced synaptic changes *in vivo*. Similar to the results of Froemke and
494 colleagues (31) for layer 2/3 cortical neurons, we observed no significant difference in the magnitude
495 of 1:1 t-LTP between the threshold repeat number (i.e., 6 repeats at 0.5 Hz) and higher repeat numbers
496 at hippocampal Schaffer collateral (SC)–CA1 synapses (25 and 70 repeats; compare Fig 1A). As for the
497 canonical protocol, we also determined the threshold for successful t-LTP induction also for the burst

498 protocol (compare Fig 1B). The observed shift of the threshold repeat number to lower values (3 instead
499 of 6 repeats for successful t-LTP induction) for the burst protocol speaks in favor of facilitated
500 postsynaptic induction by the spike train instead of single spikes used by the 1:1 protocol. Although 35
501 repeats of the burst protocol showed a tendency towards reduced magnitude of t-LTP, the efficacy of
502 3, 6 and 35 repeats of 1:4 t-LTP were not significantly different. Together these data suggest that
503 depending on the exact pattern (e.g., 1:1 vs. 1:4 paradigm) used for t-LTP induction distinct thresholds
504 for the successful number of repeats can be observed.
505
506 In cultured hippocampal neurons, Zhang and colleagues (32) showed that more than 10 repeats of their
507 1:1 STDP protocol were necessary to induce t-LTP. However, bath application of dopamine facilitated t-
508 LTP induction and reduced the number of pairings that were required at a given frequency to
509 successfully induce t-LTP (32). Since primary cultures of dissociated hippocampal neurons develop
510 synaptic connections in the absence of dopaminergic inputs, the role of endogenous DA can be
511 investigated only if t-LTP is recorded in acutely isolated hippocampal slices as performed here.
512 Interestingly, our data show that both low repeat t-LTP variants tested here are blocked when signaling
513 of endogenously released DA is inhibited (Fig 6). Our results are in line with the previously described
514 effects of exogenously added DA on t-LTP in hippocampal cultures (32). The release of endogenous DA
515 in our slices (22, 23) is therefore likely to account for the low number of repeats required for successful
516 induction of t-LTP in our study. Whether this effect is due to acute release of DA from axon terminals
517 elicited via the extracellular co-stimulation of dopaminergic afferents during t-LTP induction and test
518 stimulation or rather depends on ambient levels of DA in the slices remains to be determined.
519 Regarding the magnitude of t-LTP induced by low repeat canonical and burst protocols we, found that
520 both, 6 x 1:1 and 6 x 1:4 t-LTP, were equally successful to induce t-LTP at positive spike timings (Fig 2C).
521 Because it is reasonable to assume that 1:4 burst protocols induce longer lasting and stronger Ca^{2+}
522 elevations than 1:1 pairings, it might be expected that the time course of synaptic potentiation could
523 differ between the two protocols. However, both protocols induced t-LTP with similar onsets and rise
524 times of potentiation and also resulted in indistinguishable magnitudes of t-LTP after 1 h recording

525 (compare Fig 2D). Thus, except for the lower threshold number of repeats to elicit t-LTP (see last
526 paragraph), the burst protocol does not seem to be more effective in inducing t-LTP at SC-CA1 synapses
527 than the canonical protocol.
528 We also compared different spike timings (with negative and positive delays), to compare the full
529 capacity to induce bidirectional plasticity with low repeat protocols (Fig 2A, B). For positive pairings with
530 Δt: +25 ms we observed a similar decline (compared to Δt: +10 ms) in t-LTP magnitude as described
531 previously for higher numbers of repeats (compare 1, 30). When applying negative pairings (i.e. post
532 before pre pairings) t-LTP was absent, but we did not observe robust t-LTD for either of the two
533 protocols. While these results stress that successful induction of t-LTP is critically dependent on the
534 sequence of presynaptic and postsynaptic spiking, future studies should address under which conditions
535 low repeat t-LTD can be induced by anti-causal synaptic activation.
536
537 Mechanisms of expression of low repeat t-LTP
538 Despite the similarities described above, both low repeat protocols recruited different expression
539 mechanisms. Synaptic potentiation induced with the 6 x 1:1 protocol is most likely expressed by
540 presynaptic alterations (see below), whereas the 6 x 1:4 protocol relies on postsynaptic insertion of
541 AMPA receptors (Fig. 3). Commonly, LTP at SC-CA1 synapses that is induced by high-frequency
542 stimulation and is also thought to be expressed by a postsynaptic increase in AMPA receptor mediated
543 currents (66, 67). For STDP, however, different mechanisms of expression have been described that
544 varied between brain regions and depending on experimental conditions (see e.g., Costa et al., 2016).
545 Even at a given type of synapse (i.e. hippocampal SC-CA1) t-LTP can be expressed either pre- or
546 postsynaptically (30). At this synapse, the expression mechanism of LTP seemed to be encoded by the
547 pairing pattern used for STDP. While t-LTP induced by 70 x 1:1 stimulation was expressed via increased
548 presynaptic glutamate release, a 35 x 1:4 t-LTP was expressed via insertion of additional AMPARs by a
549 GluA1-dependent mechanism (30). However, in this previous study, we used different numbers of
550 repeats for the two t-LTP protocols (i.e. 20-35 x 1:4 and 70-100 x 1:1) to keep postsynaptic activity at an
551 equivalent level. Those previous results do not allow to distinguish whether repeat number or

552 stimulation pattern determined the site of t-LTP expression. With help of our current experiments using
553 fixed numbers of repeats for both protocols, we could now determine that the pattern of postsynaptic
554 spiking and not the repeat number influences the expression locus for t-LTP (compare Fig 3).
555
556 For the 6 x 1:1 t-LTP, the absence of an increase in AMPAR mediated currents (Pep1-TGL experiments;
557 Fig 5) and the observed increase in paired pulse ratio (PPR) after successful LTP induction, are consistent
558 with presynaptic unsilencing of glutamatergic synapses with low release probability. In contrast, other
559 presynaptic mechanisms leading to more efficient glutamate release at successfully conducting (i.e. with
560 EPSPs) synapses already before induction of LTP (18, 68, 69) are at variance with our PPR data (Fig 3A),
561 because then we should have observed a decrease rather than an increase in paired pulse facilitation
562 after t-LTP expression. Interestingly, judged by the PPR data, low and high repeat 1:1 t-LTP (compare
563 30) seem to recruit different presynaptic mechanisms for t-LTP expression. Thus, 6 x 1:1 t-LTP seems to
564 depend on presynaptic unsilencing, whereas 70 – 100 x 1:1 t-LTP leads to an increase in
565 neurotransmitter release (30). Regarding the retrograde messenger required for both types of 1:1 t-LTP
566 our data indicate that neither NO nor endocannabinoids are involved in the presynaptic expression (data
567 not shown). However, further investigating the underlying presynaptic mechanisms of 6 x 1:1 t-LTP was
568 beyond the scope of the current study. The six repeat version of our burst t-LTP protocol (6 x 1:4) seems
569 to follow the suggested classical model of SC–CA1 LTP with postsynaptic expression via insertion of new
570 AMPARs and absence of significant changes in paired pulse facilitation as previously described for high
571 repeat burst t-LTP (30). Furthermore, our experiments with Pep1-TGL clearly demonstrate the
572 importance of GluA1 containing AMPARs in expression of 6 x 1:4 t-LTP (Fig 3C).
573
574 Dependence of low repeat t-LTP induction on different sources for postsynaptic Ca^{2+} elevation
575
576 Induction of t-LTP with low repeat STDP protocols as a model to investigate physiologically relevant
577 synaptic plasticity mechanisms has just started. Accordingly, to date the contribution of different

578 sources of Ca^{2+} to its induction is unknown. Unexpectedly, our experiments revealed distinctly different
579 routes for postsynaptic Ca^{2+} elevation for the low repeat 1:1 and 1:4 protocol to induce t-LTP.
580 The results for the 6 x 1:1 t-LTP are in accordance with previous studies showing that t-LTP as well as
581 classical high frequency stimulation induced LTP at glutamatergic synapses rely on Ca^{2+} influx via
582 postsynaptic NMDA receptors (2). For STDP, NMDARs are thought to serve as coincidence detectors of
583 timed pre- and postsynaptic activation (e.g., 1, 30, 70, 71). Depending on the level of postsynaptic Ca^{2+}
584 that is reached during induction, separate signaling cascades leading to either LTP or LTD are activated
585 (cited in 13, 72, 73). For t-LTD, alternative mechanisms for coincidence detection have been described
586 (74, 75). Instead of NMDAR-mediated Ca^{2+} influx, these studies reported that either mGluRs, VGCCs or
587 IP3 gated internal Ca^{2+} stores can trigger the induction of LTD. As for LTD, also for LTP, additional
588 coincidence detectors and Ca^{2+} sources might be involved in its induction (5, VGCC: 76, IP3-sensitive
589 stores: 77, 78-80). In accordance with these previous studies, we found that 6 x 1:1 t-LTP can in addition
590 to NMDARs also be induced by Ca^{2+} entry through L-type VGCCs (Fig 4A, C).
591 In contrast to these conventional Ca^{2+} sources for the canonical low repeat t-LTP, the situation is much
592 different for 6 x 1:4 burst t-LTP. Although a requirement for postsynaptic Ca^{2+} elevation is clearly evident
593 from the BAPTA experiments (Fig 5A), Ca^{2+} entry via NMDARs or VGCCs was not involved (compare Fig
594 4B, D). Rather, our results demonstrated that the initial postsynaptic Ca^{2+} rise required for this atypical
595 form of hebbian plasticity involved group I mGluRs, RyRs and GluA2-lacking Ca^{2+}-permeable AMPAR
596 activation (compare Figs 5 and 8). Our observation that RyR-dependent Ca^{2+} release from internal stores
597 triggers 6 x 1:4 t-LTP (compare Fig 5D) suggests a role of this Ca^{2+} release pathway during induction of
598 this type of t-LTP. However, while RyRs can efficiently amplify an initially much smaller rise of
599 intracellular Ca^{2+} levels, they have not been described to be directly activated by a plasma membrane
600 resident receptor in neurons. Since neither NMDA receptors nor L-type VGCCs were involved in the
601 induction of 6 x 1:4 t-LTP (Fig 4), the initial rise in postsynaptic Ca^{2+} levels is most likely mediated by
602 either Ca^{2+} influx through GluA2 subunit deficient Ca^{2+}-permeable AMPA receptors (cp-AMPARs) into
603 the postsynaptic cell (81) or driven by activation of mGluRs (82). This is evident from our experiments
604 performed in the presence of the mGluR antagonists and the antagonist of Ca^{2+} permeable AMPARs

605 NASPM, which both completely inhibited 6 x 1:4 t-LTP (group I mGluR: Fig 5B, C, cp-AMPAR: Fig 8B, for
606 discussion of cp-AMPAR, see below).
607 Group I metabotropic GluR have indeed been described previously to be involved in some types of
608 hippocampal LTP (5), while our present results show for the first time their involvement in STDP.
609 Altogether it seems plausible that 6 x 1:4 stimulation first activates $mGluR_{1,5}$ receptors, which
610 subsequently trigger IP_3- mediated calcium release from internal stores (83). The resulting calcium rise
611 and additional Ca^{2+} influx via cp-AMPARs might than be strengthened by additional RyR mediated
612 calcium induced Ca^{2+} release to successfully boost low repeat induced burst t-LTP (compare Fig 9).
613
614 Regulation of low repeat t-LTP by dopamine receptor signaling
615
616 The accurate timing of pre- and postsynaptic activity is necessary for hebbian plasticity. In addition,
617 neuromodulator signaling critically regulates the efficacy of STDP protocols to elicit t-LTP (e.g., 17, 20,
618 21, 22, 25, 30, 32, 33, 65, 84). Since high repeat STDP in the hippocampus is regulated by dopamine (DA,
619 e.g., 23), we also investigated DAergic modulation of our two low repeat STDP variants (compare Fig 6).
620 While both low repeat t-LTP protocols were dependent on endogenous DA signaling, the
621 pharmacological profile for them was quite different. The 6 x 1:4 t-LTP was completely dependent on
622 intact D2 receptor signaling, but independent from D1 receptor signaling. This result can be easily
623 reconciled with pure D2 receptor dependent signaling being responsible for induction of the 6 x 1:4 t-
624 LTP (compare Fig 6B). However, the 6 x 1:1 t-LTP remained functional when either D1-like or D2-like
625 dopamine receptor signaling was intact. Although inhibition of D2 receptors by Sulpiride had a tendency
626 to reduce the magnitude of the 1:1 t-LTP, this effect did not reach statistical significance. Moreover,
627 while the D1 receptor inhibitor SCH23390 alone did not show any signs of 6 x 1:1 t-LTP inhibition, it was
628 nevertheless able to impair the slightly reduced t-LTP in the presence of Sulpiride down to control levels,
629 when both antagonists were co-applied (Fig 6A). The interpretation of this pharmacological profile of 6
630 x 1:1 t-LTP needs to take into consideration that D1-like and D2-like receptors do not signal exclusively
631 via altering cAMP levels (cAMP increase via D1-like receptors - or decreased via D2-like receptors; 85).

632 Rather, D5 receptors and heterodimeric D1/D2 receptors can also activate cAMP-independent PLC
633 pathways stimulating in turn IP_3/Ca^{2+}, DAG/PKC signaling, or MAPK signaling downstream of D1 receptor
634 activation and Akt kinase signaling. Also direct modulation of NMDARs and VGCCs in response to D2R
635 activation is possible (86). Although it is clear that D1-like and D2-like receptors are expressed in
636 hippocampal pyramidal neurons (86), their presence on pre- and/or postsynaptic membranes is not well
637 characterized. Consequently, the question whether the combined D1/D2 receptors dependence of the
638 1:1 t-LTP reflects rather the activation of D1/D2 heteromeric receptors, or distinct pre- vs. postsynaptic
639 expression and signaling of D1 and D2 receptors at SC-CA1 synapses needs to be addressed by future
640 experiments.
641 To interpret the combined regulation of the 6 x 1:1 t-LTP by D1 and D2 receptors it also needs to be
642 taken into consideration that D2-like receptors are generally believed to display a higher affinity for DA
643 compared to D1-like receptors (86). Therefore, the complex D1- and D2 receptor-dependent regulation
644 of 6 x 1:1 t-LTP might assure that this type of t-LTP is on the one hand regulated by the presence of DA,
645 but on the other hand remains intact at high and low DA concentrations. On the same vein, this co-
646 regulation could assure that slowly rising ambient DA levels created by tonic firing of DAergic neurons
647 are equally effective in regulating 6 x 1:1 t-LTP as much faster rising DA concentrations during phasic
648 firing.
649 Such a change in DA release was indeed shown in recordings of midbrain neurons, where activity of
650 DAergic neurons switches from tonic to phasic burst activity resulting in locally distinct levels of secreted
651 DA in the target regions (87). Local DA concentration differences can then result in different DA-
652 dependent effects, with high affinity D2-like receptors being activated by low and slowly rising
653 extracellular DA levels, while low affinity D1 receptors are only activated by local DA peaks.
654 For our STDP experiments where DAergic input fibers are most likely co-activated during SC stimulation,
655 we observed similar activity-dependent recruitment of different DA receptors. While D1 receptor-
656 dependent effects were activated by 70-100 stimulations (22 and compare Fig 6C), D1/D2 receptors or
657 pure D2 receptor mediated processes were already activated by six presynaptic co-stimulations of
658 DAergic fibers (compare Fig 6). Taking into account that D2-like receptors (i.e. D2, D3 and D4 receptors)

659 are classically thought to inhibit LTP by decreasing cAMP/PKA signaling (88, 89), D2-like receptor driven
660 t-LTP processes might indeed be activated by $G_{\beta\gamma}$ signaling independent of cAMP pathways. As
661 mentioned above, $G_{\beta\gamma}$ signaling also blocks L-type and N-type VGCCs (85) and D2 receptor signaling can
662 yield Ca^{2+} release from internal stores - two mechanisms that might account for the uncommon type of
663 calcium source required for the induction of our 6 x 1:4 t-LTP (compare Figs 4 and 5).
664
665 Dependence of low repeat t-LTP on BDNF/TrkB signaling
666
667 Brain-derived neurotrophic factor (BDNF) is well known for its important role in mediating long-lasting
668 changes of synaptic plasticity (reviewed in e.g., 16, 90, 91, 92). Moreover, BDNF is also involved in
669 regulating STDP (28-30). For hippocampal SC-CA1 synapses it was shown that BDNF is secreted from
670 postsynaptic CA1 neurons in response to 20-35 repeats of a 1:4 STDP protocol mediating
671 postsynaptically expressed t-LTP via postsynaptic TrkB receptor activation (30). Interestingly, the results
672 of the present study revealed, that neither of the two low repeat t-LTP variants depends on BDNF
673 induced TrkB signaling (compare Fig 7). This finding was not unexpected since release of endogenous
674 BDNF has been reported previously to require more prolonged barrages of AP firing than just 6 repeats
675 of short AP (burst) firing at 0.5 Hz (compare 29, 30, 93). Nevertheless, the 6 x 1:1 t-LTP was significantly
676 inhibited in the presence of the Trk kinase inhibitor K252a. The mode of application and the K252a
677 concentration used in these experiments has been shown previously to selectively interfere with Trk
678 tyrosine kinase function in neurons (see e.g., 19, 30, 94). Therefore, the most straight forward
679 interpretation of the K252a-dependent inhibition of the 6 x 1:1 t-LTP is that transactivation of TrkB
680 receptors - independent of BDNF - might be involved in this type of low repeat t-LTP. In fact, such a
681 transactivation by dopamine has been reported previously for striatal neurons (95). Likewise,
682 transactivation of TrkB receptors was also reported for other G-protein coupled receptors mediating
683 adenosine or PACAP signaling (96). At hippocampal mossy fiber synapses zinc influx through NMDA
684 receptors has been shown to mediate activation of Src family kinases causing subsequent TrkB

685 activation (55, but see 56, 57). Additional experiments are clearly required to clarify the possible role of
686 transactivation routes of TrkB receptors in low repeat t-LTP.
687
688 Function of GluA2-lacking Ca^{2+} permeable AMPA receptors in low repeat t-LTP
689
690 Interestingly, both variants of low repeat t-LTP were strictly dependent on activation of GluA2-lacking
691 calcium-permeable (cp-)AMPA receptors (Fig 8). In these experiments, NASPM was present in the ACSF
692 from the start of the recording to assure complete inhibition of cp-AMPARs during t-LTP induction. In
693 CA1 neurons, cp-AMPARs were described to be absent from postsynaptic membranes during basal
694 synaptic stimulation. Rather, they were reported to transiently insert into the postsynaptic membrane
695 after tetanic LTP stimulation to allow sustained Ca^{2+} influx into the postsynaptic neuron after LTP
696 induction, thereby facilitating expression of late LTP (reviewed in 61). A role of cp-AMPARs in STDP has
697 thus far not been reported. Additional experiments will be required to determine the time course of
698 activity-dependent cp-AMPAR incorporation during induction of low repeat t-LTP into the postsynaptic
699 membrane. Furthermore, it needs to be determined how cp-AMPAR mediated Ca^{2+} influx is
700 orchestrated with mGluR- and RyR-dependent Ca^{2+} elevation for induction of low repeat 6 x 1:4 t-LTP.
701 Likewise, the co-operation of cp-AMPARs with NMDAR- and VGCC-dependent Ca^{2+} elevations for
702 inducing 6 x 1:1 t-LTP needs to be investigated.
703 Alternatively, cp-AMPARs might be involved in DA-dependent priming of synapses for
704 delayed/retroactive reinforcement of LTP or silent eligibility traces (e.g., 97, 98-100). Such mechanisms
705 might also be involved in the signaling mechanisms employed by our low repeat t-LTP protocols (6 x 1:1
706 and 6 x 1:4), since both variants of t-LTP show a clear dependence on DA signaling and on cp-AMPARs
707 (compare Figs 6 and 8).
708
709 In summary, we used two different low repeat STDP protocols at SC-CA1 synapses to record synaptic
710 plasticity at the single cell level in postsynaptic CA1 neurons (i.e. t-LTP). We found that, dependent on
711 stimulation pattern and repeat number, distinct signaling and expression mechanisms are activated by

712 the canonical and the burst low repeat paradigm. From our experiments, we can conclude that even
713 with the same experimental setup, age and species, multiple types of synaptic plasticity mechanisms
714 can coexist at a given type of synapse. This plethora of coexisting plasticity mechanisms for
715 strengthening synaptic transmission seems to be ideally suited to empower the hippocampus to fulfill
716 its multiplexed functions in memory storage.
717
718 Material and Methods
719
720 Preparation of hippocampal slices
721 Horizontal hippocampal slices (350 µm thickness) were prepared from 4 weeks old male wild type
722 C57BL/6J (Charles River), $BDNF^{+/-}$ or littermate control mice (101; all animals bred on a C57Bl/6J
723 background), according to the ethical guidelines for the use of animal in experiments, and were carried
724 out in accordance with the European Committee Council Directive (2010/63/EU) and approved by the
725 local animal care committee (Landesverwaltungsamt Sachsen-Anhalt).
726 Briefly, mice were decapitated under deep anesthesia with forene (Isofluran CP, cp-pharma, Germany)
727 and the brain was rapidly dissected and transferred into ice-cold artificial cerebrospinal fluid (ACSF)
728 cutting solution (125 mM NaCl, 2.5 mM KCl, 0.8 mM NaH_2PO_4, 25 mM $NaHCO_3$, 25 mM Glucose, 6 mM
729 $MgCl_2$, 1 mM $CaCl_2$; pH 7.4; 300-303 mOsmol/kg), saturated with 95% O_2 and 5% CO_2. Blocks from both
730 hemispheres containing the hippocampus and the entorhinal cortex were sectioned with a vibratome
731 (VT 1200 S, Leica, Germany). Slices were incubated for 35 min at 32°C in a handmade interface chamber
732 containing carboxygenated ACSF cutting solution and then transferred to room temperature (~21°C) for
733 at least 1 hour before the recording started. Whole cell patch-clamp recordings were performed in
734 submerged slices in a recording chamber with continuous perfusion (1-2 ml per min) of pre-warmed (30
735 ± 0.2°C) carboxygenated physiological ACSF solution (125 mM NaCl, 2.5 mM KCl, 0.8 mM NaH_2PO_4, 25
736 mM $NaHCO_3$, 25 mM Glucose, 1 mM $MgCl_2$, 2 mM $CaCl_2$; pH 7.4; 300-303 mOsmol/kg). For all
737 experiments, 100 µM Picrotoxin ($GABA_A$ blocker) was added to ACSF solution. Epileptiform activity by
738 activation of recurrent CA3 synapses was prevented by a cut between CA3 and CA1 subfields (compare

739 30). To reduce the amount of inhibitors in some of the experiments (e.g. application of NASPM) we used
740 a micro-perfusion pump-driven solution recycling system (Bioptechs Delta T Micro-Perfusion pump high
741 flow, ChromaPhor, Germany) to limit the volume of solution for incubation of slices (19). Respective
742 matched control experiments were performed under identical conditions to assure that the
743 microperfusion recycling of ACSF alone did not affect t-LTP.
744
745 Electrophysiological recordings
746 Whole cell patch-clamp recordings were performed on pyramidal neurons in the CA1 subregion of the
747 intermediate hippocampus under visual control with infrared DIC-videomicroscopy (RT-SE series;
748 Diagnostic instruments, Michigan, USA). The pipettes (resistance 5-7 MΩ) were filled with internal
749 solution containing (in mM): 10 HEPES, 20 KCl, 115 potassium gluconate, 0.00075 $CaCl_2$, 10 Na
750 phosphocreatine, 0.3 Na-GTP, and 4 Mg-ATP (pH 7.4, 285-290 mOsmol/kg). Cells were held at -70 mV
751 in current clamp or voltage clamp (liquid junction potential of +10 mV of internal solution was corrected)
752 with an EPC-8 patch clamp amplifier (HEKA, Lamprecht, Germany). Extracellular stimulation of the
753 Schaffer collateral (SC) fibers to generate an excitatory postsynaptic potential (EPSP, at 0.05Hz) was
754 induced by glass stimulation electrodes (resistance 0.7 – 0.9 MΩ) positioned in Stratum radiatum (SR)
755 of the CA1 subregion. The stimulus intensity was adjusted to evoke responses with amplitudes of 4-5
756 mV corresponding to 30-50% of maximal EPSP amplitudes. Stimulus duration was set to 0.7 ms with
757 intensities ranging between 90 to 700 µA.
758
759 Induction of Spike timing-dependent plasticity
760 Spike timing-dependent plasticity (STDP) was induced by pairing of an individual EPSP, generated by
761 extracellular stimulation of SC, with a single action potential (AP) or with a burst of 4 APs (frequency 200
762 Hz) induced by somatic current injection (2 ms; 1 nA) through the recording electrode (30). Pairings of
763 postsynaptic EPSP and APs were usually performed with a time interval of +10 ms, and were repeated
764 2-70 times at a frequency of 0.5 Hz to elicit t-LTP. In some experiments, either longer time windows
765 (positive spike timings: Δt= 17-25 ms) were used to test t-LTP at longer Δt or short negative spike timings

766 (Δt= -15ms) were used when trying to elicit t-LTD. EPSPs were monitored every 20 s (i.e., 0.05 Hz) for
767 10 min baseline and then 30 min or 60 min after t-LTP (or t-LTD) induction. Unpaired stimulation of 4
768 postsynaptic APs instead of a full STDP protocol were performed (i.e., 6x 0:4) in a subset of cells that
769 served as controls. In another set of cells, we assessed possible spontaneous changes in synaptic
770 transmission (stimulation at 0.05 Hz for 40 min) in the absence of any STDP stimulation. These
771 recordings served as negative controls (designated 0:0 controls).
772 To investigate whether a rise of postsynaptic Ca^{2+} concentration is required for induction of t-LTP under
773 our conditions, we applied the Ca^{2+} chelator BAPTA (10 mM, Sigma, Germany) via the patch pipette
774 solution in the recorded postsynaptic neuron. NMDA receptor (R) dependency was tested by application
775 of an NMDAR antagonist (APV 50 µM, DL-2-Amino-5-phosphonopentanoic acid, Tocris, Germany) in the
776 bath solution. The contribution of L-type voltage gated Ca^{2+} channel activation to t-LTP was evaluated
777 with bath applied Nifedipine (25 µM, Sigma, Germany). To interfere with group I metabotropic
778 glutamate receptor (mGluR) signaling we used bath application of either the $mGlu_1$ receptor antagonist
779 YM298198 (1 µM, Tocris, Germany) or the $mGluR_5$ receptor antagonist MPEP (10 µM, Tocris, Germany)
780 alone, or both blocker simultaneously. Intracellular infusion of ryanodine (100 µM, Tocris, Germany)
781 was used to block ryanodine receptors of internal calcium stores. To investigate the possible role of zinc-
782 dependent transactivation of TrkB we applied the cell-permeable zinc chelator TPEN (10 µM, Tocris,
783 Germany) in the bath solution during t-LTP induction with the 6 x 1:1 protocol. Where appropriate,
784 respective controls were performed with ACSF or internal solution containing the same final
785 concentration of DMSO as used for the drug containing solution (i.e. solvent controls).
786
787 We investigated dopaminergic neuromodulation of STDP by bath application of specific antagonists for
788 dopamine D1-like (SCH23390, SCH; 10 µM, Sigma) and dopamine D2-like receptors (Sulpiride, Sulp; 10
789 µM, Sigma). The contribution of BDNF/TrkB signaling was tested by bath application of either the
790 tyrosine kinase inhibitor K252a (200 nM, Alomone labs, Israel) or a scavenger of endogenous BDNF
791 (recombinant human TrkB Fc chimera, R&D Systems, Germany). For scavenging of BDNF, slices were
792 pre-incubated for at least 3h with 5µg/ml TrkB-Fc, and subsequent recordings were performed in the

793 presence of 100 ng/ml TrkB-Fc (compare 30). Positive controls were recorded in slices kept under the
794 same regime, but without the addition of TrkB-Fc. Matched controls for the K252a experiments were
795 performed in the presence of the vehicle (0.05% DMSO, vehicle control). To test low repeat t-LTP under
796 conditions of chronic 50% BDNF reduction, we used heterozygous BDNF $^{+/-}$ mice and respective wildtype
797 littermates as described previously (30).
798 The contribution of activity-dependent incorporation of GluA1 subunit containing AMPA receptors to
799 expression of low repeat t-LTP was verified by postsynaptic application of Pep1-TGL (100 µM, Tocris,
800 Germany) via the patch pipette solution. To investigate a possible role of GluA2 lacking calcium
801 permeable (cp-) AMPA receptors, we use bath applied NASPM (1-Naphtyl acetyl spermine
802 trihydrochloride, 100 µM, Tocris, Germany).
803
804 Data acquisition and Data Analysis
805 Data were filtered at 3 kHz using a patch clamp amplifier (EPC-8, HEKA, Germany) connected to a LiH8+8
806 interface and digitized at 10 kHz using PATCHMASTER software (HEKA, Germany). Data analysis was
807 performed with Fitmaster software (HEKA, Germany). All experiments were performed in the current
808 clamp mode, except for paired pulse ratio (PPR) that was recorded in the voltage clamp mode at -70 mV
809 holding potential, and AMPA/NMDA receptor current ratios that were recorded in voltage clamp at -70
810 mV and -20 mV holding potential. Input resistance was monitored by hyperpolarizing current steps (250
811 ms; 20 pA), elicited prior to evoked EPSP responses. The average slope calculated from 10 min control
812 recording (baseline) were set to 100% and all subsequent EPSP slopes of a cell were expressed as
813 percentage of baseline slopes. Synaptic strength was calculated from the mean EPSP slopes 20-30 min
814 (or 50-60 min) after STDP induction, divided by the mean EPSP slope measured during 10 min before
815 STDP stimulation (baseline). Spike timing intervals (i.e. *Δt,* ms) were measured as the time between
816 onset of the evoked EPSP and the peak of the first action potential. Cells were only included for analysis
817 if the initial resting membrane potential (RMP) was between -55 and -70 mV. Cells were excluded when
818 the input resistance varied more than 25% over the entire experiment. Furthermore, traces showing
819 visible “run-up” or “run-down” during baseline recording were excluded.

820 AMPA/NMDA receptor mediated current ratios were calculated from the peak current amplitudes of
821 the fast AMPA receptor mediated components evoked at a holding potential of -70 mV divided by the
822 amplitudes of the NMDAR mediated slow current components measured after 50 ms of the onset of
823 the EPSCs at a holding potential of -20 mV. Selectivity of this procedure for AMPAR and NMDAR
824 mediated currents was confirmed by bath application of either 50 µM APV or 10 µM NBQX in some
825 experiments (compare 30).
826 For analysis of presynaptic short-term plasticity before and after t-LTP induction, paired pulse facilitation
827 was recorded in voltage clamp mode at a holding potential of -70 mV, and the paired pulse ratio (PPR)
828 was determined by dividing the peak current amplitudes of the second EPSC by the first EPSC at an inter-
829 stimulus interval of 50 ms.
830 To verify independent expression of the two low repeat paradigms, we performed an occlusion
831 approach. Here we subsequently activate first the 6 x 1:1 and 25 min later the 6 x 1:4 t-LTP in the same
832 cell and compared the change in synaptic strength by the two protocols.
833
834 Statistics
835 Statistical analysis was performed using GraphPad Prism version 6.0 (GraphPad Software, USA) or JMP
836 8 (SAS Institute Inc., USA). Pooled data of experiments from at least three different animals are
837 expressed as mean ± SEM. Paired and unpaired two tailed t-tests were used for data with normal
838 distribution. Otherwise nonparametric Mann-Whitney U-test was applied. Multiple comparisons were
839 assessed with a one-way analysis of variance (ANOVA), followed by a post hoc t-test Dunnet's test or
840 Kruskal-Wallis test, followed by post hoc Dunn's test for parametric and nonparametric data. A p-value
841 <0.05 was set as level of significance and is indicated by an asterisk. The actual statistic procedures used
842 for each experiment are mentioned in the text. The respective number of experiments (n) and the
843 number of animals (N) is reported in the figure legends.
844
845 Acknowledgments:

The project was funded by the federal state of Saxony-Anhalt and the “European Regional Developmental Fund (ERDF 2014-2020), Project: Center for Behavioral Brain Sciences (CBBS) FKS: ZS/2016/04/78113; by the federal state Saxony-Anhalt and the European Structural and Investment Funds (ESF, 2014-2020), project number ZS/2016/08/80645 and by the DFG ED 280/1-1 and SFB779/B06. The authors thank Regina Ziegler for her help.

CRediT

Conceptualization: VL, EE; Methodology: VL, EE and EC-P; Investigation: EC-P, BK, GQ with help by EE and SB; Writing: EE, VL, with help by EC-P; Funding Acquisition: VL, EE; Resources: VL; Supervision: VL, EE.

858 References

859 1. Bi GQ, Poo MM. Synaptic modifications in cultured hippocampal neurons: dependence on spike
860 timing, synaptic strength, and postsynaptic cell type. J Neurosci. 1998;18(24):10464-72.
861 2. Malenka RC, Bear MF. LTP and LTD: an embarrassment of riches. Neuron. 2004;44(1):5-21.
862 3. Bliss TV, Cooke SF. Long-term potentiation and long-term depression: a clinical perspective.
863 Clinics (Sao Paulo). 2011;66 Suppl 1:3-17.
864 4. Lynch MA. Long-term potentiation and memory. Physiol Rev. 2004;84(1):87-136.
865 5. Wang H, Ardiles AO, Yang S, Tran T, Posada-Duque R, Valdivia G, et al. Metabotropic Glutamate
866 Receptors Induce a Form of LTP Controlled by Translation and Arc Signaling in the Hippocampus. J
867 Neurosci. 2016;36(5):1723-9.
868 6. Bliss TV, Lomo T. Long-lasting potentiation of synaptic transmission in the dentate area of the
869 anaesthetized rabbit following stimulation of the perforant path. J Physiol. 1973;232(2):331-56.
870 7. Tonegawa S, Morrissey MD, Kitamura T. The role of engram cells in the systems consolidation
871 of memory. Nat Rev Neurosci. 2018;19(8):485-98.
872 8. Herring BE, Nicoll RA. Long-Term Potentiation: From CaMKII to AMPA Receptor Trafficking. Annu
873 Rev Physiol. 2016;78:351-65.
874 9. Lalanne T, Oyrer J, Farrant M, Sjostrom PJ. Synapse Type-Dependent Expression of Calcium-
875 Permeable AMPA Receptors. Front Synaptic Neurosci. 2018;10:34.
876 10. Pinar C, Fontaine CJ, Trivino-Paredes J, Lottenberg CP, Gil-Mohapel J, Christie BR. Revisiting the
877 flip side: Long-term depression of synaptic efficacy in the hippocampus. Neurosci Biobehav Rev.
878 2017;80:394-413.
879 11. Otto T, Eichenbaum H, Wiener SI, Wible CG. Learning-related patterns of CA1 spike trains
880 parallel stimulation parameters optimal for inducing hippocampal long-term potentiation.
881 Hippocampus. 1991;1(2):181-92.
882 12. Bi GQ, Poo MM. Synaptic modification by correlated activity: Hebb's postulate revisited. Annu
883 Rev Neurosci. 2001;24:139-66.

884 13. Caporale N, Dan Y. Spike timing-dependent plasticity: a Hebbian learning rule. Annu Rev
885 Neurosci. 2008;31:25-46.
886 14. Markram H, Gerstner W, Sjostrom PJ. A history of spike-timing-dependent plasticity. Front
887 Synaptic Neurosci. 2011;3:4.
888 15. Feldman DE. The spike-timing dependence of plasticity. Neuron. 2012;75(4):556-71.
889 16. Edelmann E, Lessmann V, Brigadski T. Pre- and postsynaptic twists in BDNF secretion and action
890 in synaptic plasticity. Neuropharmacology. 2014;76 Pt C:610-27.
891 17. Edelmann E, Cepeda-Prado E, Lessmann V. Coexistence of Multiple Types of Synaptic Plasticity
892 in Individual Hippocampal CA1 Pyramidal Neurons. Front Synaptic Neurosci. 2017;9:7.
893 18. Costa RP, Mizusaki BE, Sjostrom PJ, van Rossum MC. Functional consequences of pre- and
894 postsynaptic expression of synaptic plasticity. Philos Trans R Soc Lond B Biol Sci. 2017;372(1715).
895 19. Meis S, Endres T, Lessmann V. Postsynaptic BDNF signalling regulates long-term potentiation at
896 thalamo-amygdala afferents. J Physiol. 2012;590(Pt 1):193-208.
897 20. Seol GH, Ziburkus J, Huang S, Song L, Kim IT, Takamiya K, et al. Neuromodulators control the
898 polarity of spike-timing-dependent synaptic plasticity. Neuron. 2007;55(6):919-29.
899 21. Pawlak V, Kerr JN. Dopamine receptor activation is required for corticostriatal spike-timing-
900 dependent plasticity. J Neurosci. 2008;28(10):2435-46.
901 22. Edelmann E, Lessmann V. Dopamine Modulates Spike Timing-Dependent Plasticity and Action
902 Potential Properties in CA1 Pyramidal Neurons of Acute Rat Hippocampal Slices. Front Synaptic
903 Neurosci. 2011;3:6.
904 23. Edelmann E, Lessmann V. Dopamine regulates intrinsic excitability thereby gating successful
905 induction of spike timing-dependent plasticity in CA1 of the hippocampus. Front Neurosci. 2013;7:25.
906 24. Liu Y, Cui L, Schwarz MK, Dong Y, Schluter OM. Adrenergic Gate Release for Spike Timing-
907 Dependent Synaptic Potentiation. Neuron. 2017;93(2):394-408.
908 25. Edelmann E, Lessmann V. Dopaminergic innervation and modulation of hippocampal networks.
909 Cell Tissue Res. 2018;373(3):711-27.

910 26. Mu Y, Poo MM. Spike timing-dependent LTP/LTD mediates visual experience-dependent
911 plasticity in a developing retinotectal system. Neuron. 2006;50(1):115-25.
912 27. Pattwell SS, Bath KG, Perez-Castro R, Lee FS, Chao MV, Ninan I. The BDNF Val66Met
913 Polymorphism Impairs Synaptic Transmission and Plasticity in the Infralimbic Medial Prefrontal Cortex.
914 J Neurosci. 2012;32(7):2410-21.
915 28. Sivakumaran S, Mohajerani MH, Cherubini E. At immature mossy-fiber-CA3 synapses, correlated
916 presynaptic and postsynaptic activity persistently enhances GABA release and network excitability via
917 BDNF and cAMP-dependent PKA. J Neurosci. 2009;29(8):2637-47.
918 29. Lu H, Park H, Poo MM. Spike-timing-dependent BDNF secretion and synaptic plasticity. Philos
919 Trans R Soc Lond B Biol Sci. 2014;369(1633):20130132.
920 30. Edelmann E, Cepeda-Prado E, Franck M, Lichtenecker P, Brigadski T, Lessmann V. Theta Burst
921 Firing Recruits BDNF Release and Signaling in Postsynaptic CA1 Neurons in Spike-Timing-Dependent LTP.
922 Neuron. 2015;86(4):1041-54.
923 31. Froemke RC, Tsay IA, Raad M, Long JD, Dan Y. Contribution of individual spikes in burst-induced
924 long-term synaptic modification. J Neurophysiol. 2006;95(3):1620-9.
925 32. Zhang JC, Lau PM, Bi GQ. Gain in sensitivity and loss in temporal contrast of STDP by
926 dopaminergic modulation at hippocampal synapses. Proc Natl Acad Sci U S A. 2009;106(31):13028-33.
927 33. Cui Y, Paille V, Xu H, Genet S, Delord B, Fino E, et al. Endocannabinoids mediate bidirectional
928 striatal spike-timing dependent plasticity. J Physiol. 2015.
929 34. Cui Y, Prokin I, Xu H, Delord B, Genet S, Venance L, et al. Endocannabinoid dynamics gate spike-
930 timing dependent depression and potentiation. Elife. 2016;5:e13185.
931 35. Pike FG, Meredith RM, Olding AW, Paulsen O. Rapid report: postsynaptic bursting is essential
932 for 'Hebbian' induction of associative long-term potentiation at excitatory synapses in rat hippocampus.
933 J Physiol. 1999;518 (Pt 2):571-6.
934 36. Buchanan KA, Mellor JR. The development of synaptic plasticity induction rules and the
935 requirement for postsynaptic spikes in rat hippocampal CA1 pyramidal neurones. J Physiol. 2007;585(Pt
936 2):429-45.

937 37. Schulz PE, Cook EP, Johnston D. Changes in paired-pulse facilitation suggest presynaptic
938 involvement in long-term potentiation. J Neurosci. 1994;14(9):5325-37.
939 38. Kleschevnikov AM, Sokolov MV, Kuhnt U, Dawe GS, Stephenson JD, Voronin LL. Changes in
940 paired-pulse facilitation correlate with induction of long-term potentiation in area CA1 of rat
941 hippocampal slices. Neuroscience. 1997;76(3):829-43.
942 39. Morita D, Rah JC, Isaac JT. Incorporation of inwardly rectifying AMPA receptors at silent
943 synapses during hippocampal long-term potentiation. Philos Trans R Soc Lond B Biol Sci.
944 2014;369(1633):20130156.
945 40. Lee HK, Kirkwood A. AMPA receptor regulation during synaptic plasticity in hippocampus and
946 neocortex. Semin Cell Dev Biol. 2011;22(5):514-20.
947 41. Chater TE, Goda Y. The role of AMPA receptors in postsynaptic mechanisms of synaptic
948 plasticity. Front Cell Neurosci. 2014;8:401.
949 42. Hayashi Y, Shi SH, Esteban JA, Piccini A, Poncer JC, Malinow R. Driving AMPA receptors into
950 synapses by LTP and CaMKII: requirement for GluR1 and PDZ domain interaction. Science.
951 2000;287(5461):2262-7.
952 43. Shi S, Hayashi Y, Esteban JA, Malinow R. Subunit-specific rules governing AMPA receptor
953 trafficking to synapses in hippocampal pyramidal neurons. Cell. 2001;105(3):331-43.
954 44. Nicoll RA, Malenka RC. Contrasting properties of two forms of long-term potentiation in the
955 hippocampus. Nature. 1995;377(6545):115-8.
956 45. Tigaret CM, Olivo V, Sadowski J, Ashby MC, Mellor JR. Coordinated activation of distinct Ca(2+)
957 sources and metabotropic glutamate receptors encodes Hebbian synaptic plasticity. Nat Commun.
958 2016;7:10289.
959 46. Balschun D, Manahan-Vaughan D, Wagner T, Behnisch T, Reymann KG, Wetzel W. A specific role
960 for group I mGluRs in hippocampal LTP and hippocampus-dependent spatial learning. Learn Memory.
961 1999;6(2):138-52.

962 47. Neyman S, Manahan-Vaughan D. Metabotropic glutamate receptor 1 (mGluR1) and 5 (mGluR5)
963 regulate late phases of LTP and LTD in the hippocampal CA1 region in vitro. Eur J Neurosci.
964 2008;27(6):1345-52.
965 48. Gao J, Voss AA, Pessah IN, Lauer FT, Penning TM, Burchiel SW. Ryanodine receptor-mediated
966 rapid increase in intracellular calcium induced by 7,8-benzo(a)pyrene quinone in human and murine
967 leukocytes. Toxicol Sci. 2005;87(2):419-26.
968 49. Missale C, Nash SR, Robinson SW, Jaber M, Caron MG. Dopamine receptors: from structure to
969 function. Physiol Rev. 1998;78(1):189-225.
970 50. Dubovyk V, Manahan-Vaughan D. Less means more: The magnitude of synaptic plasticity along
971 the hippocampal dorso-ventral axis is inversely related to the expression levels of plasticity-related
972 neurotransmitter receptors. Hippocampus. 2018;28(2):136-50.
973 51. Papaleonidopoulos V, Kouvaros S, Papatheodoropoulos C. Effects of endogenous and
974 exogenous D1/D5 dopamine receptor activation on LTP in ventral and dorsal CA1 hippocampal
975 synapses. Synapse. 2018;72(8):e22033.
976 52. Hagena H, Manahan-Vaughan D. Dopamine D1/D5, But not D2/D3, Receptor Dependency of
977 Synaptic Plasticity at Hippocampal Mossy Fiber Synapses that Is Enabled by Patterned Afferent
978 Stimulation, or Spatial Learning. Front Synaptic Neurosci. 2016;8:31.
979 53. Endres T, Lessmann V. Age-dependent deficits in fear learning in heterozygous BDNF knock-out
980 mice. Learn Mem. 2012;19(12):561-70.
981 54. Psotta L, Rockahr C, Gruss M, Kirches E, Braun K, Lessmann V, et al. Impact of an additional
982 chronic BDNF reduction on learning performance in an Alzheimer mouse model. Front Behav Neurosci.
983 2015;9:58.
984 55. Huang YZ, Pan E, Xiong ZQ, McNamara JO. Zinc-mediated transactivation of TrkB potentiates the
985 hippocampal mossy fiber-CA3 pyramid synapse. Neuron. 2008;57(4):546-58.
986 56. Helgager J, Huang YZ, McNamara JO. Brain-derived neurotrophic factor but not vesicular zinc
987 promotes TrkB activation within mossy fibers of mouse hippocampus in vivo. J Comp Neurol.
988 2014;522(17):3885-99.

989 57. Huang YZ, McNamara JO. Mutual regulation of Src family kinases and the neurotrophin receptor
990 TrkB. J Biol Chem. 2010;285(11):8207-17.
991 58. Kauer JA, Malenka RC. LTP: AMPA receptors trading places. Nat Neurosci. 2006;9(5):593-4.
992 59. Plant K, Pelkey KA, Bortolotto ZA, Morita D, Terashima A, McBain CJ, et al. Transient
993 incorporation of native GluR2-lacking AMPA receptors during hippocampal long-term potentiation. Nat
994 Neurosci. 2006;9(5):602-4.
995 60. Man HY. GluA2-lacking, calcium-permeable AMPA receptors--inducers of plasticity? Curr Opin
996 Neurobiol. 2011;21(2):291-8.
997 61. Park P, Kang H, Sanderson TM, Bortolotto ZA, Georgiou J, Zhuo M, et al. The Role of Calcium-
998 Permeable AMPARs in Long-Term Potentiation at Principal Neurons in the Rodent Hippocampus. Front
999 Synaptic Neurosci. 2018;10:42.
1000 62. Wittenberg GM, Wang SS. Malleability of spike-timing-dependent plasticity at the CA3-CA1
1001 synapse. J Neurosci. 2006;26(24):6610-7.
1002 63. Couey JJ, Meredith RM, Spijker S, Poorthuis RB, Smit AB, Brussaard AB, et al. Distributed network
1003 actions by nicotine increase the threshold for spike-timing-dependent plasticity in prefrontal cortex.
1004 Neuron. 2007;54(1):73-87.
1005 64. Carlisle HJ, Fink AE, Grant SG, O'Dell TJ. Opposing effects of PSD-93 and PSD-95 on long-term
1006 potentiation and spike timing-dependent plasticity. J Physiol. 2008;586(Pt 24):5885-900.
1007 65. Yang K, Dani JA. Dopamine D1 and D5 receptors modulate spike timing-dependent plasticity at
1008 medial perforant path to dentate granule cell synapses. J Neurosci. 2014;34(48):15888-97.
1009 66. Granger AJ, Nicoll RA. Expression mechanisms underlying long-term potentiation: a
1010 postsynaptic view, 10 years on. Philos T R Soc B. 2014;369(1633).
1011 67. Nicoll RA. Expression mechanisms underlying long-term potentiation: a postsynaptic view.
1012 Philos T R Soc B. 2003;358(1432):721-6.
1013 68. Zucker RS, Regehr WG. Short-term synaptic plasticity. Annu Rev Physiol. 2002;64:355-405.
1014 69. Kaeser PS, Regehr WG. Molecular mechanisms for synchronous, asynchronous, and
1015 spontaneous neurotransmitter release. Annu Rev Physiol. 2014;76:333-63.

1016 70. Debanne D, Gahwiler BH, Thompson SM. Long-term synaptic plasticity between pairs of
1017 individual CA3 pyramidal cells in rat hippocampal slice cultures. J Physiol. 1998;507 (Pt 1):237-47.
1018 71. Feldman DE. Timing-based LTP and LTD at vertical inputs to layer II/III pyramidal cells in rat
1019 barrel cortex. Neuron. 2000;27(1):45-56.
1020 72. Lisman J. A mechanism for the Hebb and the anti-Hebb processes underlying learning and
1021 memory. Proc Natl Acad Sci U S A. 1989;86(23):9574-8.
1022 73. Artola A, Singer W. Long-term depression of excitatory synaptic transmission and its relationship
1023 to long-term potentiation. Trends Neurosci. 1993;16(11):480-7.
1024 74. Bender VA, Bender KJ, Brasier DJ, Feldman DE. Two coincidence detectors for spike timing-
1025 dependent plasticity in somatosensory cortex. J Neurosci. 2006;26(16):4166-77.
1026 75. Fino E, Venance L. Spike-timing dependent plasticity in the striatum. Front Synaptic Neurosci.
1027 2010;2:6.
1028 76. Magee JC, Johnston D. A synaptically controlled, associative signal for Hebbian plasticity in
1029 hippocampal neurons. Science. 1997;275(5297):209-13.
1030 77. Takechi H, Eilers J, Konnerth A. A new class of synaptic response involving calcium release in
1031 dendritic spines. Nature. 1998;396(6713):757-60.
1032 78. Dudman JT, Tsay D, Siegelbaum SA. A role for synaptic inputs at distal dendrites: instructive
1033 signals for hippocampal long-term plasticity. Neuron. 2007;56(5):866-79.
1034 79. Nanou E, Scheuer T, Catterall WA. Calcium sensor regulation of the CaV2.1 Ca2+ channel
1035 contributes to long-term potentiation and spatial learning. Proc Natl Acad Sci U S A.
1036 2016;113(46):13209-14.
1037 80. Wiera G, Nowak D, van Hove I, Dziegiel P, Moons L, Mozrzymas JW. Mechanisms of NMDA
1038 Receptor- and Voltage-Gated L-Type Calcium Channel-Dependent Hippocampal LTP Critically Rely on
1039 Proteolysis That Is Mediated by Distinct Metalloproteinases. J Neurosci. 2017;37(5):1240-56.
1040 81. Suzuki T, Miura M, Nishimura K, Aosaki T. Dopamine-dependent synaptic plasticity in the striatal
1041 cholinergic interneurons. J Neurosci. 2001;21(17):6492-501.

1042 82. Kaar A, Rae MG. Metabotropic glutamate receptor-mediated cyclic ADP ribose signalling.
1043 Biochem Soc Trans. 2015;43(3):405-9.
1044 83. Jong YJ, Sergin I, Purgert CA, O'Malley KL. Location-dependent signaling of the group 1
1045 metabotropic glutamate receptor mGlu5. Mol Pharmacol. 2014;86(6):774-85.
1046 84. Cassenaer S, Laurent G. Conditional modulation of spike-timing-dependent plasticity for
1047 olfactory learning. Nature. 2012;482(7383):47-52.
1048 85. Tritsch NX, Sabatini BL. Dopaminergic modulation of synaptic transmission in cortex and
1049 striatum. Neuron. 2012;76(1):33-50.
1050 86. Beaulieu JM, Gainetdinov RR. The physiology, signaling, and pharmacology of dopamine
1051 receptors. Pharmacol Rev. 2011;63(1):182-217.
1052 87. Rosen ZB, Cheung S, Siegelbaum SA. Midbrain dopamine neurons bidirectionally regulate CA3-
1053 CA1 synaptic drive. Nat Neurosci. 2015;18(12):1763-71.
1054 88. Otmakhov N, Lisman JE. Postsynaptic application of a cAMP analogue reverses long-term
1055 potentiation in hippocampal CA1 pyramidal neurons. J Neurophysiol. 2002;87(6):3018-32.
1056 89. Otmakhova NA, Otmakhov N, Mortenson LH, Lisman JE. Inhibition of the cAMP pathway
1057 decreases early long-term potentiation at CA1 hippocampal synapses. J Neurosci. 2000;20(12):4446-51.
1058 90. Lessmann V, Gottmann K, Malcangio M. Neurotrophin secretion: current facts and future
1059 prospects. Prog Neurobiol. 2003;69(5):341-74.
1060 91. Park H, Poo MM. Neurotrophin regulation of neural circuit development and function. Nat Rev
1061 Neurosci. 2013;14(1):7-23.
1062 92. Gottmann K, Mittmann T, Lessmann V. BDNF signaling in the formation, maturation and
1063 plasticity of glutamatergic and GABAergic synapses. Exp Brain Res. 2009;199(3-4):203-34.
1064 93. Balkowiec A, Katz DM. Cellular mechanisms regulating activity-dependent release of native
1065 brain-derived neurotrophic factor from hippocampal neurons. J Neurosci. 2002;22(23):10399-407.
1066 94. Schildt S, Endres T, Lessmann V, Edelmann E. Acute and chronic interference with BDNF/TrkB-
1067 signaling impair LTP selectively at mossy fiber synapses in the CA3 region of mouse hippocampus.
1068 Neuropharmacology. 2013;71:247-54.

1069 95. Iwakura Y, Nawa H, Sora I, Chao MV. Dopamine D1 receptor-induced signaling through TrkB
1070 receptors in striatal neurons. J Biol Chem. 2008;283(23):15799-806.
1071 96. Rajagopal R, Chen ZY, Lee FS, Chao MV. Transactivation of Trk neurotrophin receptors by G-
1072 protein-coupled receptor ligands occurs on intracellular membranes. J Neurosci. 2004;24(30):6650-8.
1073 97. Brzosko Z, Schultz W, Paulsen O. Retroactive modulation of spike timing-dependent plasticity
1074 by dopamine. Elife. 2015;4.
1075 98. He K, Huertas M, Hong SZ, Tie X, Hell JW, Shouval H, et al. Distinct Eligibility Traces for LTP and
1076 LTD in Cortical Synapses. Neuron. 2015;88(3):528-38.
1077 99. Shindou T, Shindou M, Watanabe S, Wickens J. A silent eligibility trace enables dopamine-
1078 dependent synaptic plasticity for reinforcement learning in the mouse striatum. Eur J Neurosci.
1079 2019;49(5):726-36.
1080 100. Gerstner W, Lehmann M, Liakoni V, Corneil D, Brea J. Eligibility Traces and Plasticity on
1081 Behavioral Time Scales: Experimental Support of NeoHebbian Three-Factor Learning Rules. Front Neural
1082 Circuits. 2018;12:53.
1083 101. Korte M, Carroll P, Wolf E, Brem G, Thoenen H, Bonhoeffer T. Hippocampal long-term
1084 potentiation is impaired in mice lacking brain-derived neurotrophic factor. Proc Natl Acad Sci U S A.
1085 1995;92(19):8856-60.
1086

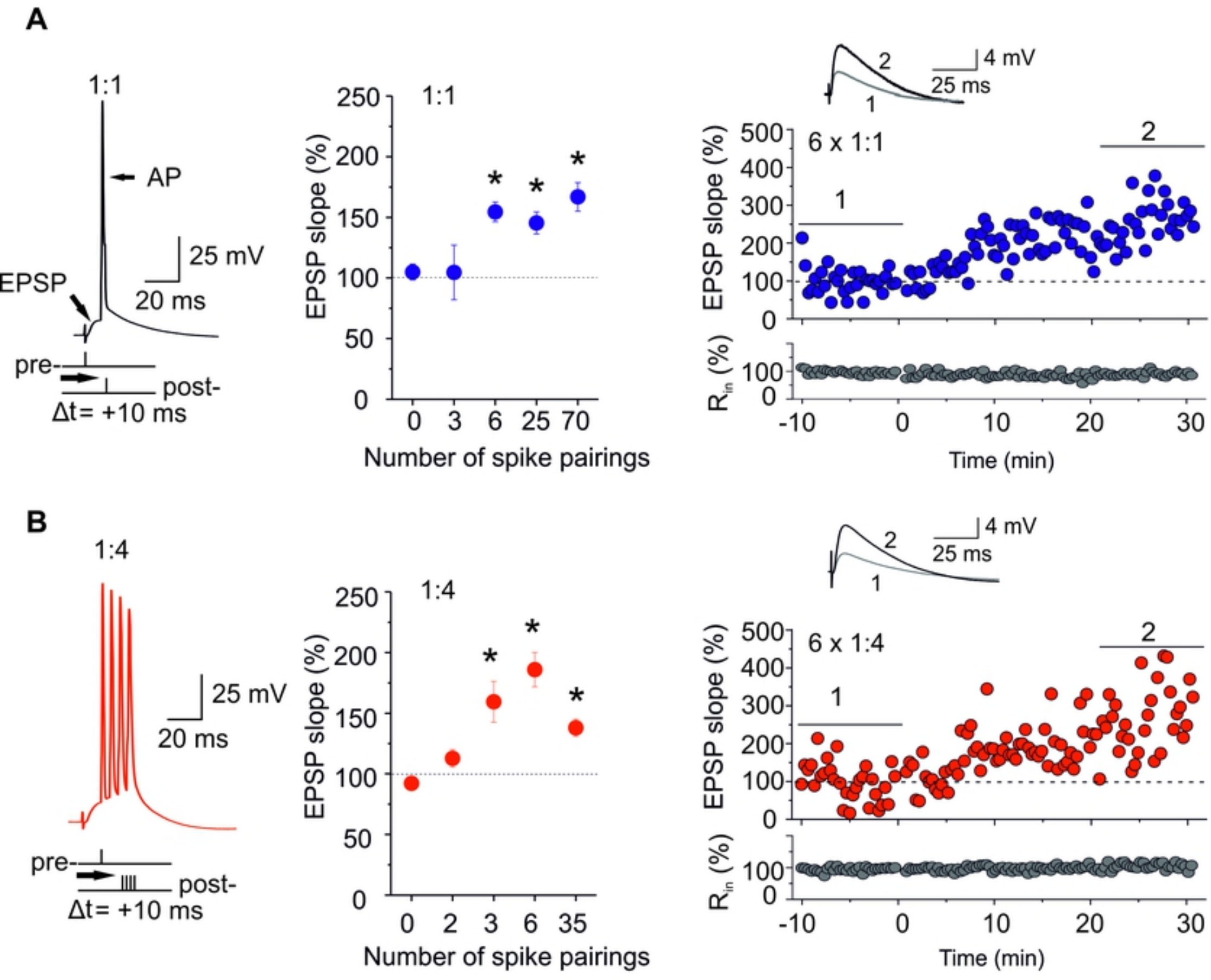

Cepeda-Prado E *et al*, Figure 1

Figure 1

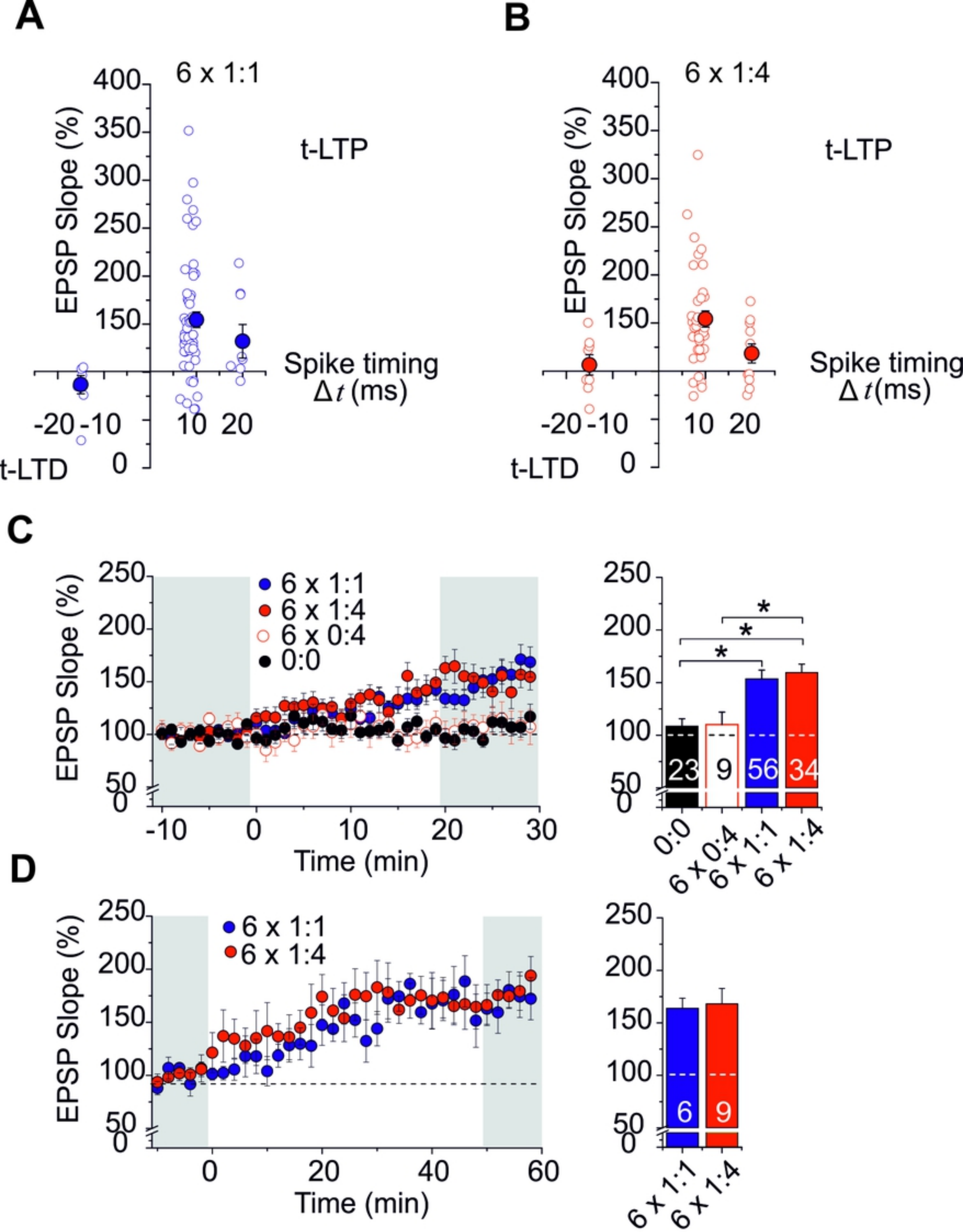

Cepeda-Prado E *et al*, Figure 2

Figure 2

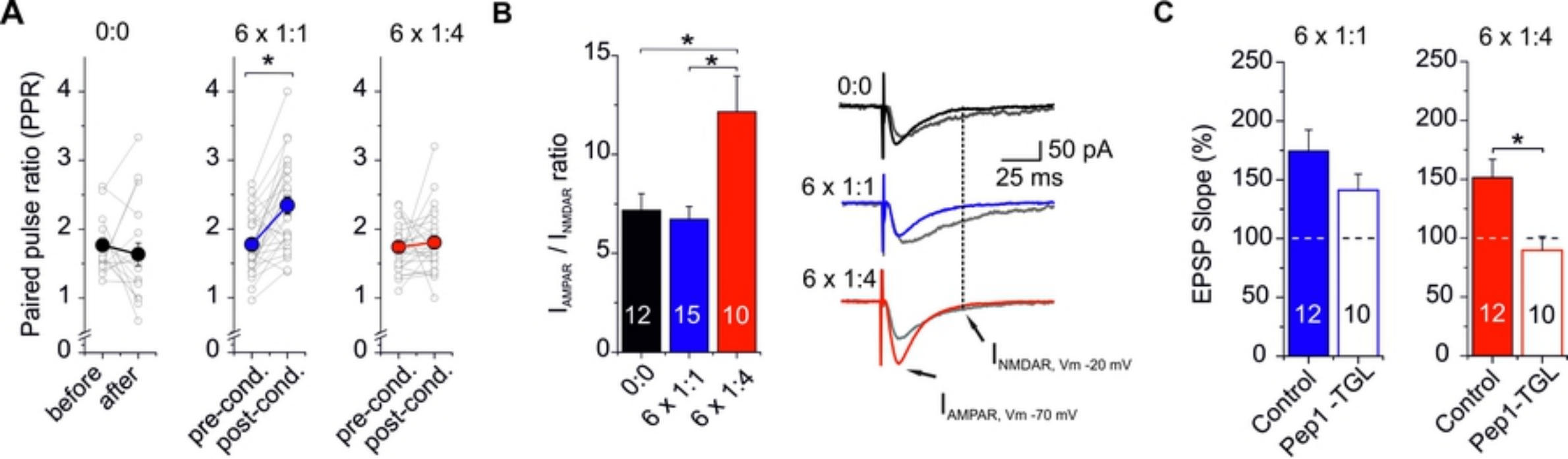

Cepeda-Prado E *et al*, Figure 3

Figure 3

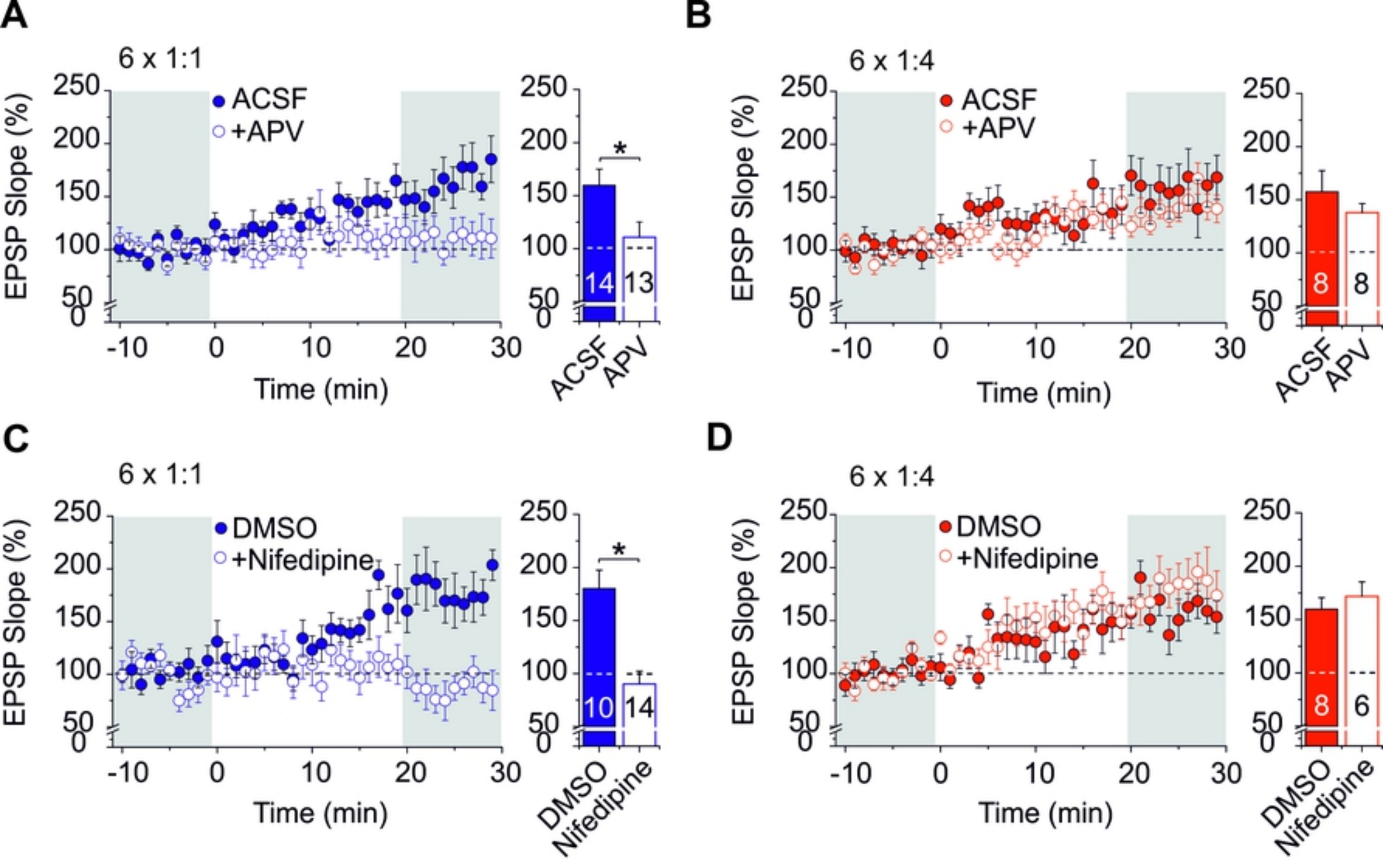

Cepeda-Prado E *et al*, Figure 4

Figure 4

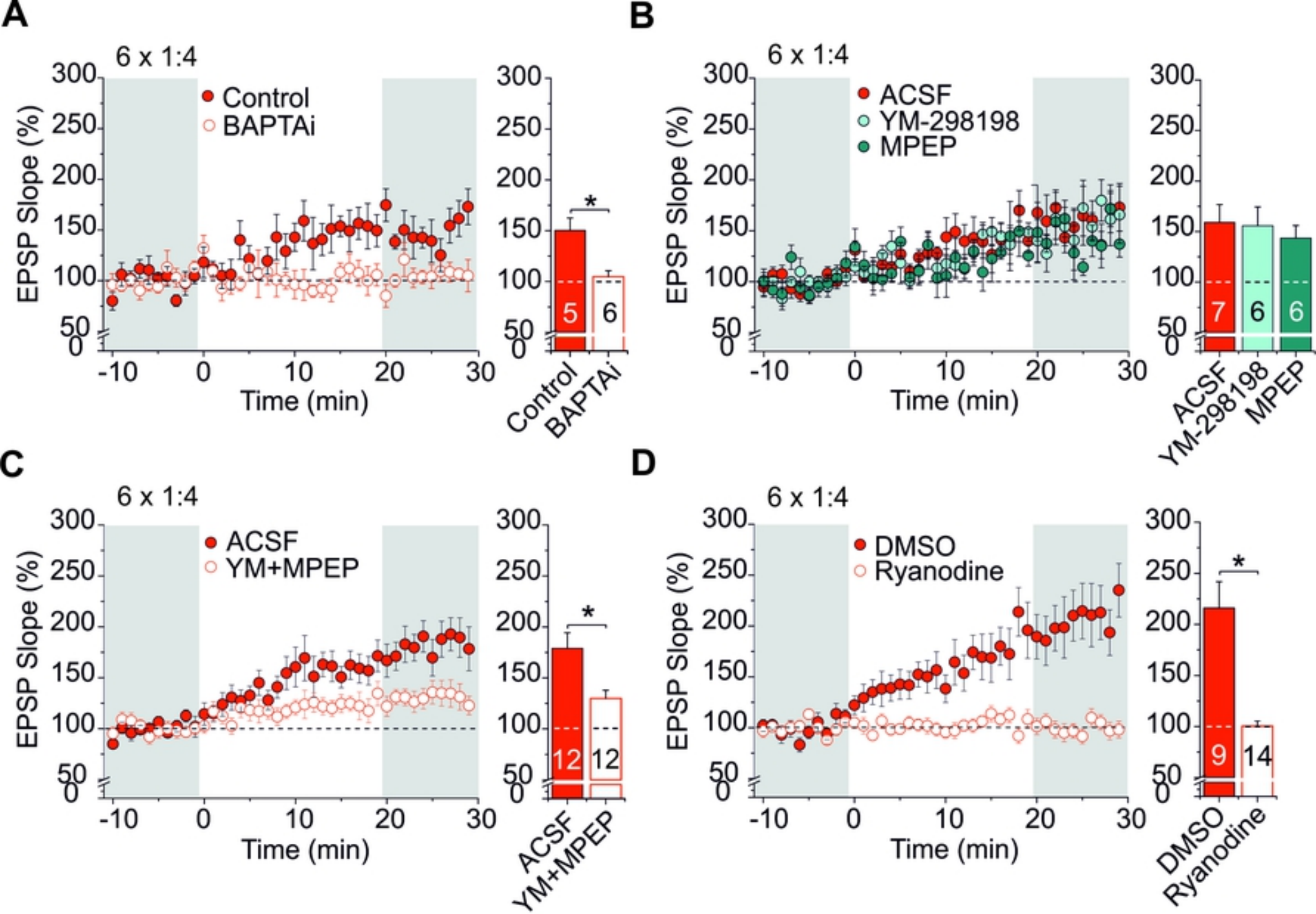

Cepeda-Prado E *et al*, Figure 5

Figure 5

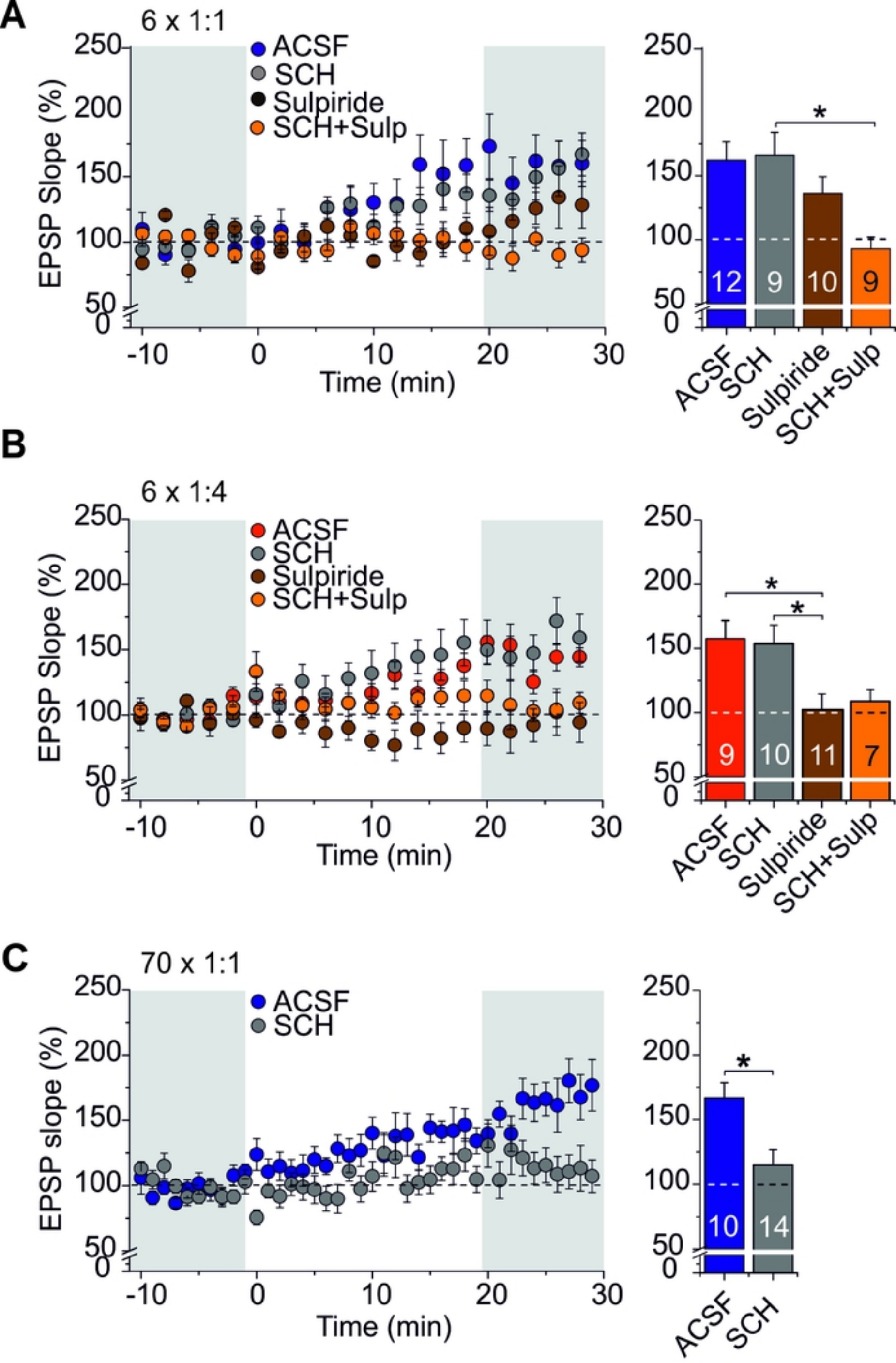

Cepeda-Prado E *et al*, Figure 6

Figure 6

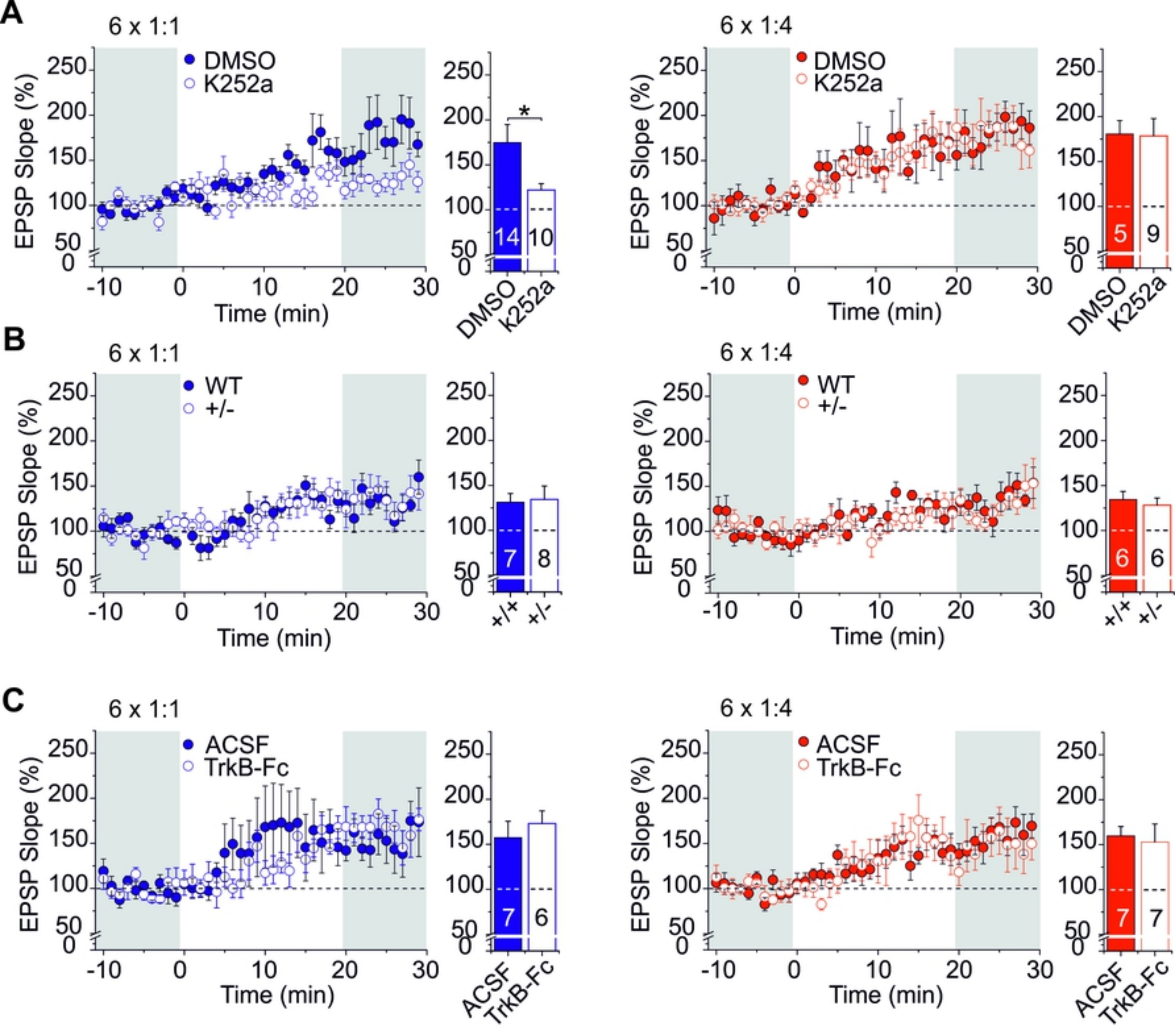

Cepeda-Prado E *et al*, Figure 7

Figure 7

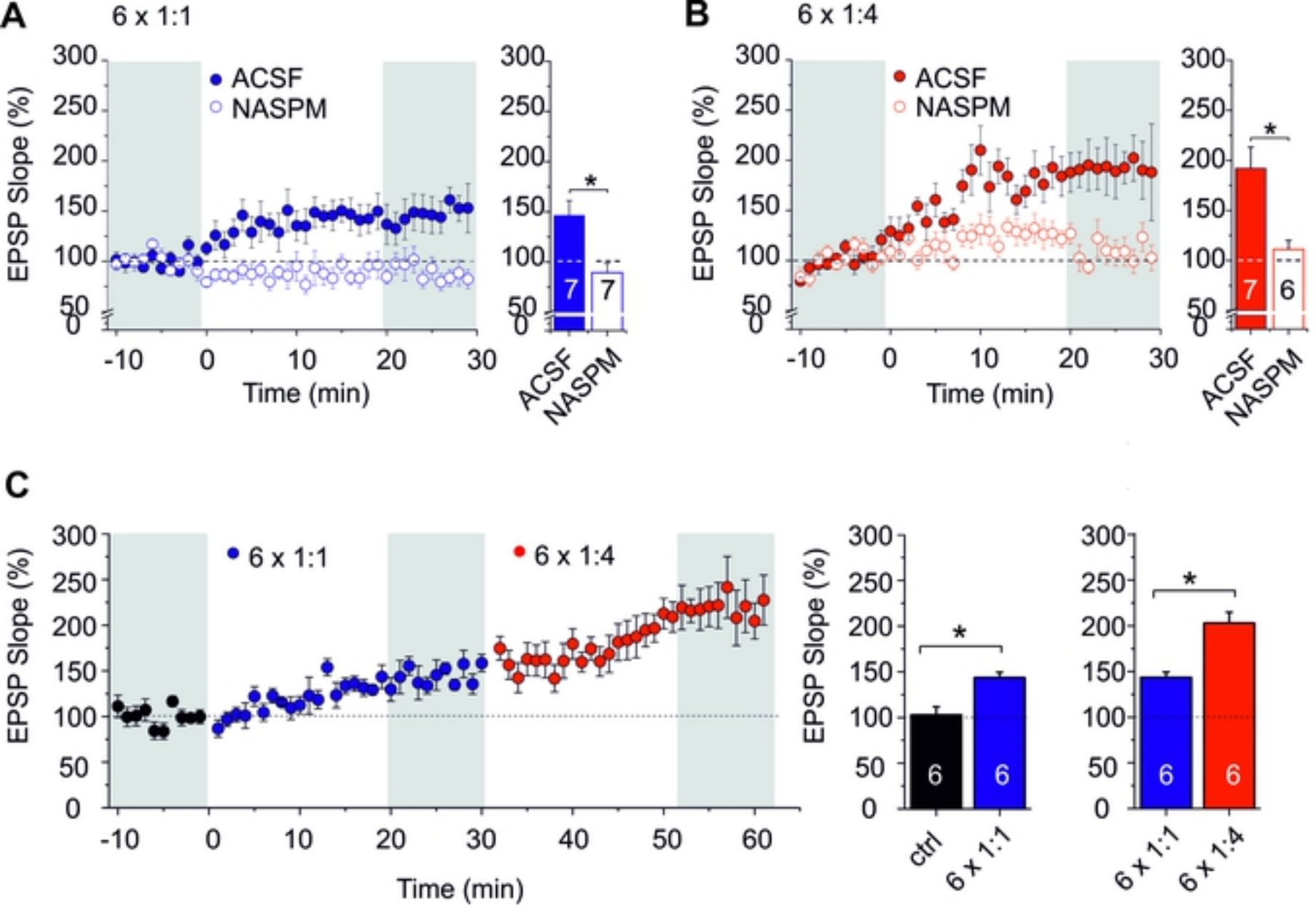

Cepeda-Prado E *et al*, Figure 8

Figure 8

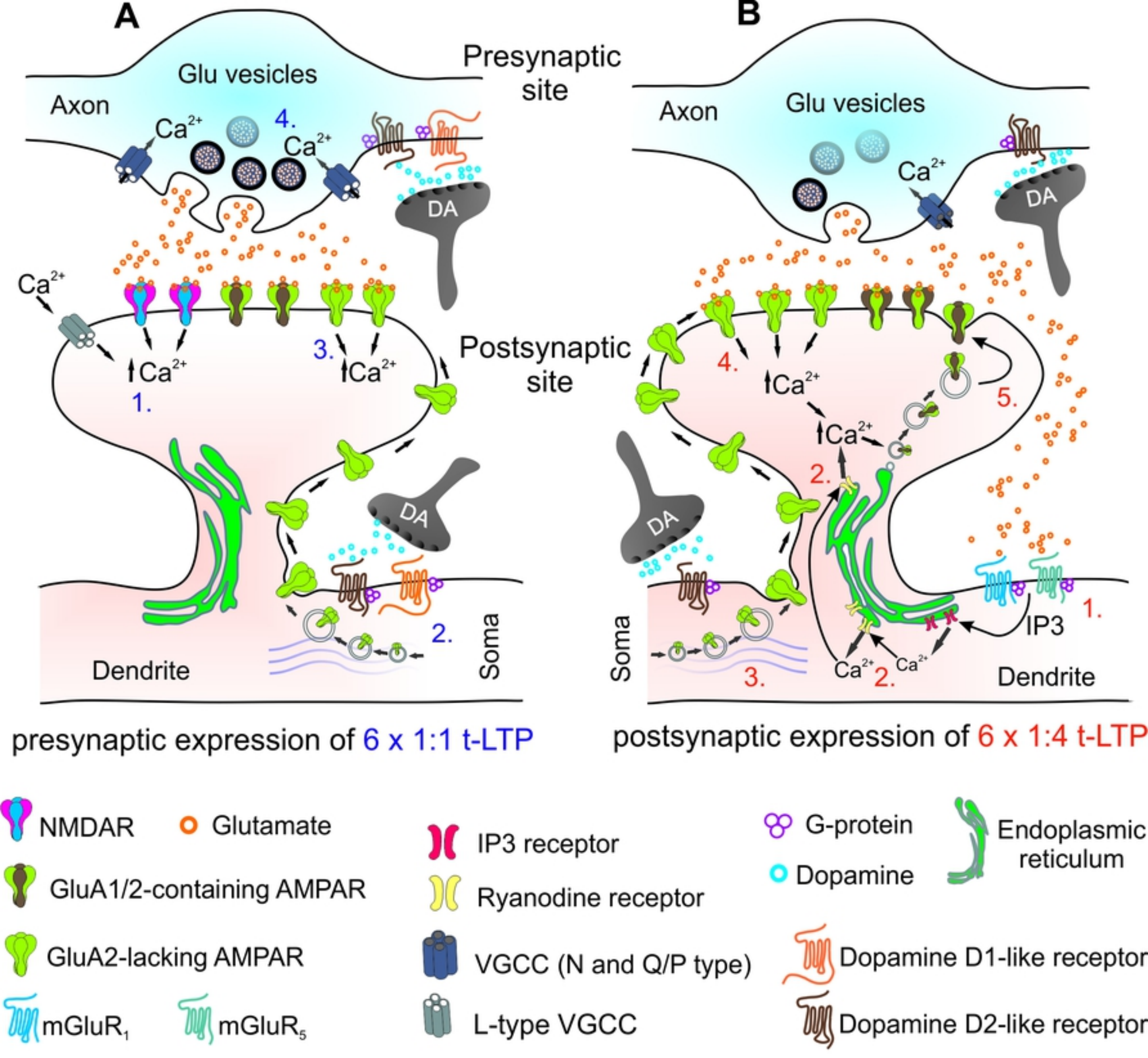

Cepeda-Prado E *et al*, Figure 9

Figure 9